A Preclinical Model of Obesity-Independent Metabolic Syndrome for Studying the Effects of Novel Antidiabetic Therapy Beyond Glycemic Control

Jonathan Mochel[1], Jessica Ward[2], Thomas Blondel[3], Debosmita Kundu[2], Maria Merodio[2], Claudine Zemirline[3], Emilie Guillot[3], Ryland Giebelhaus[4], Paulina de la Mata[4], Chelsea Iennarella-Servantez[2], April Blong[2], Seo Lin Nam[4], James Harynuk[4], Jan Suchodolski[5], Asta Tvarijonaviciute[6], José Joaquín Cerón[6], Agnes Bourgois-Mochel[1], Faiez Zannad[7], Naveed Sattar[8], and Karin Allenspach[1]

[1]University of Georgia
[2]Iowa State University
[3]Ceva Santé Animale
[4]University of Alberta
[5]Texas A&M University
[6]University of Murcia
[7]Universite de Lorraine
[8]University of Glasgow

November 17, 2023

Abstract

Accumulating data from several large, placebo-controlled studies suggests that sodium-glucose transporter 2 (SGLT-2) inhibitors and glucagon-like peptide 1 receptor (GLP-1) receptor agonists offer therapeutic benefits in the management of cardiovascular diseases, regardless of the patient's diabetic status. In addition to their effects on glucose excretion, SGLT2 inhibitors have a positive impact on systemic metabolism. The aim of this study was to establish a non-invasive preclinical model of metabolic syndrome (MetS) to investigate the effects of novel antidiabetic therapies beyond glucose reduction, independent of obesity. Eighteen healthy adult Beagle dogs were fed an isocaloric Western diet (WD) for ten weeks. Biospecimens were collected at baseline (BAS1) and after ten weeks of WD feeding (BAS2) for measurement of blood pressure (BP), serum chemistry, lipoprotein profiling, fasting blood glucose, glucagon, insulin, NT-proBNP, BUN, creatinine, angiotensins, oxidative stress biomarkers, serum, urine and fecal metabolomics. Differences between BAS1 and BAS2 were analyzed using non-parametric Wilcoxon signed-rank testing with continuity correction. The isocaloric WD model induced significant variations in several markers of MetS, including elevated BP, increased glucose levels, and reduced HDL-cholesterol. It also caused an increase in circulating NT-proBNP levels, a decrease in serum bicarbonate levels, and significant changes in general metabolism, lipids, and biogenic amines. Short-term, isocaloric feeding with a WD in dogs replicates key biological features of MetS while also causing low-grade metabolic acidosis and elevating natriuretic peptides. These findings support the use of the WD canine model for studying the metabolic effects of new antidiabetic therapies independent of obesity.

A Preclinical Model of Obesity-Independent Metabolic Syndrome for Studying the Effects of Novel Antidiabetic Therapy Beyond Glycemic Control

Jonathan P. Mochel[1,2], Jessica L. Ward[3], Thomas Blondel[4], Debosmita Kundu[2], Maria M. Merodio[3], Claudine Zemirline[4], Emilie Guillot[4], Ryland T. Giebelhaus[5], Paulina de la Mata[5], Chelsea A. Iennarella-Servantez[2], April Blong[3], Seo Lin Nam[5], James J. Harynuk[5], Jan Suchodolski[6], Asta Tvarijonaviciute[7], José Joaquín Cerón[7], Agnes Bourgois-Mochel[1,2], Faiez Zannad[8], Naveed Sattar[9] and Karin Allenspach[1,2]

[1]Precision One Health Initiative, Department of Pathology, University of Georgia College of Veterinary Medicine, 30602 Athens, GA (USA).

[2]SMART Pharmacology, Iowa State University, 50011-1250 Ames, IA (USA).

[3]Veterinary Clinical Sciences, Iowa State University, 50011-1250 Ames, IA (USA).

[4]Ceva Santé Animale, 33500 Libourne (France).

[5]The Metabolomics Innovation Centre, T6G 2G2 Edmonton (Canada). Department of Chemistry, University of Alberta, T6G 2G2 Edmonton (Canada).

[6]Gastrointestinal Laboratory, Texas A&M University, 77845 College Station, TX (USA).

[7]Interdisciplinary Laboratory of Clinical Analysis (Interlab-UMU), Veterinary School, Regional Campus of International Excellence 'Campus Mare Nostrum', University of Murcia, Campus de Espinardo s/n, 30100, Espinardo, Murcia (Spain).

[8]Université de Lorraine, Centre d'Investigations Cliniques Plurithématique 1433 and Inserm U1116, CHRU Nancy, FCRIN INI-CRCT, 54000 Nancy (France).

[9]School of Cardiovascular and Metabolic Health, BHF Glasgow Cardiovascular Research Centre, University of Glasgow, 126 University Place, Glasgow, G12 8TA (Scotland).

Corresponding author

Jonathan P. Mochel, DVM, MS, Ph.D, DECVPT, Professor of Systems Pharmacology

501 D.W. Brooks Drive, Athens, GA 30602

Email: jpmochel@uga.edu

Running Title: Western Diet-Induced Metabolic Dysfunction in Dogs.

Keywords: Western Diet; Metabolic Syndrome; Cardiorenal Metabolic Diseases; One Health.

ABSTRACT

Background and Purpose

Accumulating data from several large, placebo-controlled studies suggests that sodium-glucose transporter 2 (SGLT-2) inhibitors and glucagon-like peptide 1 receptor receptor agonists offer therapeutic benefits in the management of cardiovascular diseases, regardless of the patient's diabetic status. In addition to their effects on glucose excretion, SGLT-2 inhibitors have a positive impact on systemic metabolism. The aim of this study was to establish a non-invasive preclinical model of metabolic syndrome (***MetS***) to investigate the effects of novel antidiabetic therapies beyond glucose reduction, independent of obesity.

Experimental Approach

Eighteen healthy adult Beagle dogs were fed an isocaloric Western diet (WD) for ten weeks. Biospecimens were collected at baseline (***BAS1***) and after ten weeks of WD feeding (***BAS2***) for measurement of blood pressure (BP), serum chemistry, lipoprotein profiling, blood glucose, glucagon, insulin, NT-proBNP, angiotensins, oxidative stress biomarkers, serum, urine and fecal metabolomics. Differences between ***BAS1*** and ***BAS2*** were analyzed using non-parametric Wilcoxon signed-rank testing.

Key Results

The isocaloric WD model induced significant variations in several markers of ***MetS***, including elevated BP, increased glucose levels, and reduced HDL-cholesterol. It also caused an increase in circulating NT-proBNP levels, a decrease in serum bicarbonate levels, and significant changes in general metabolism, lipids, and biogenic amines.

Conclusions and Implications

Short-term, isocaloric feeding with a WD in dogs replicates key biological features of ***MetS*** while also causing low-grade metabolic acidosis and elevating natriuretic peptides. These findings support the use of the WD canine model for studying the metabolic effects of new antidiabetic therapies independent of obesity.

INTRODUCTION

Type 2 diabetes mellitus (T2DM) is a chronic metabolic disorder characterized by hyperglycemia resulting from insulin resistance and impaired insulin secretion (Diabetes Prevention Program Research Group, 2015). Recent data from the National Diabetes Statistics Report indicate that 37.3 million Americans suffer from T2DM (Center for Disease Control and Prevention, 2023). In addition, the economic cost of diabetes and prediabetes was estimated to have reached $322 billion in the U.S in 2012. Current protocols for the management of T2DM include lifestyle modifications, the administration of oral antidiabetic agents, and insulin therapy. However, these approaches often prove insufficient in achieving adequate glycemic control and mitigating the progression of concomitant cardiovascular and renal complications.

Two classes of drugs that are showing significant promise in the treatment of T2DM are glucagon-like peptide 1 receptor (GLP-1) receptor agonists and sodium-glucose co-transporter 2 (SGLT-2) inhibitors. SGLT-2 inhibitors, such as dapagliflozin, velagliflozin, and empagliflozin, work by inhibiting glucose reabsorption in the kidneys, thus increasing urinary glucose excretion and lowering blood glucose levels (Cowie and Fisher, 2020). These drugs have proven more effective in reducing glycated hemoglobin (HbA1c) levels compared to conventional antidiabetic therapy (Cowie and Fisher, 2020). In addition to their effects on glucose excretion, SGLT-2-inhibitors positively impact systemic metabolism by reducing inflammation and oxidative stress, shifting metabolism towards ketone body production, promoting autophagy and suppressing glycation end-product signaling (Packer, 2020).

Evidence from numerous large-scale, placebo-controlled studies suggests that SGLT-2 inhibitors may offer benefits in the treatment of cardiovascular diseases, regardless of the patient's diabetic status (Zinman et al., 2015; Neal et al., 2017; Birkeland et al., 2017; Persson et al., 2018; McMurray et al., 2019; Inzucchi et al., 2020; Packer et al., 2020; Butler et al., 2021). Notably, the EMPA-REG OUTCOME trial showed that empagliflozin reduced the risk of major adverse cardiovascular events (MACE) by 14% and cardiovascular death by 38% in patients with type 2 diabetes and established cardiovascular disease (Zinman et al., 2015). Similarly, the CANVAS and CANVAS-R

trials established that canagliflozin reduced the risk of MACE by 14% and heart failure hospitalization by 33% in patients with T2DM and a high risk of cardiovascular disease (Neal et al., 2017). SGLT-2 inhibitors have also demonstrated potential in improving renal outcomes in patients with T2DM and diabetic kidney disease. The CREDENCE trial showed that canagliflozin reduced the risk of end-stage kidney disease, doubling of serum creatinine, renal or cardiovascular death by 30% in patients with T2DM and established diabetic kidney disease (Perkovic et al., 2019). These findings provide further evidence of the multifaceted benefits of SGLT-2 inhibitors beyond glycemic control and support their therapeutic use in modulating cardiorenal metabolic diseases.

Unlike SGLT-2 inhibitors, the benefit of GLP-1 agonists in improving cardiovascular outcomes for patients with heart failure or those without T2DM has not yet been fully established (Khan et al. 2020). Ongoing studies are currently examining the potential cardiovascular benefits of semaglutide in patients with T2DM (NCT03914326, SOUL), as well as in overweight or obese patients (NCT03574597, SELECT). Additionally, a recent randomized, double-blind, placebo-controlled trial (NCT04788511, STEP-HFpEF) has shown promising results, suggesting that semaglutide can improve both symptoms and physical function in patients with heart failure with preserved systolic function and obesity (Kosiborod et al., 2023). Alongside GLP-1 receptor agonists, the effectiveness of newer combinations with glucagon agonists and/or glucose-dependent insulinotropic peptide (GIP) agonists is also being studied in regards to MACE in patients with T2DM (NCT04255433, SURPASS CVOT).

As defined by the American Heart Association (Ndumele et al., 2023), cardiovascular-kidney-metabolic health reflects the interaction between metabolic risk factors, chronic kidney disease, and the cardiovascular system. The pleiotropic effects of SGLT-2 inhibitors and GLP-1 agonists provide an opportunity to target several cardiorenal metabolic disorders. This can be achieved experimentally using a disease model that replicates key features of metabolic syndrome (***MetS***), a cluster of risk factors that include obesity, dyslipidemia, hypertension, and insulin resistance. Collectively, these factors increase the risk of developing cardiorenal diseases, metabolic dysfunction-associated steatohepatitis and T2DM (Packer, 2020; Newsome and Ambery, 2023) (**Figure 1**). Implementing such a model would enable mechanistic studies to explore the metabolic

effects of novel antidiabetic therapy beyond glycemic control. Concurrently, it could generate pivotal preliminary data that could guide the development of similar therapeutic applications in veterinary medicine, such as canine congestive heart failure, chronic kidney disease, or systemic hypertension under the One Health paradigm (Mochel et al., 2015; Mochel and Danhof, 2015; Schneider et al., 2018; Mochel et al., 2019).

Previous studies suggest that consistently overfeeding dogs with high-calorie Western diets (WDs) leads to obesity and ***MetS***, regardless of the diet composition (Moinard et al., 2020; Xue et al., 2022). Indeed, prior studies investigating the effects of WDs in dogs have primarily focused on metabolic dysfunction related to obesity (Tvarijonaviciute et al., 2012b; Peña et al., 2014; Moinard et al., 2020; Sun et al., 2023; Vecchiato et al., 2023). Within the context of obesity, both dogs and humans exhibit a redistribution of adipose tissue characterized by an increase in visceral fat, as opposed to subcutaneous fat. This shift is independently associated with the onset of ***MetS***. In addition, most clinical studies demonstrating therapeutic benefits from dapagliflozin and empagliflozin on cardiorenal outcome measures include a majority of *non*-obese patients (McMurray et al., 2019; Wheeler et al. 2020; Butler et al., 2021; Oyama et al., 2022; EMPA-KIDNEY Collaborative Group, 2023). Recently, a study conducted by Adamson et al. and published in the *European Journal of Heart Failure* has unequivocally established that the efficacy of dapagliflozin for heart failure patients with reduced ejection fraction remains consistent regardless of their body mass index (Adamson et al., 2021). There is, therefore, a clear rationale for studying the pharmacodynamic effects of these therapeutic drugs in a metabolic dysfunction model that is not dependent on obesity.

In a preliminary study conducted by our consortium, dogs fed a WD for about a month presented with elevated fasting bile acids, cholesterol, and blood pressure compared to control (Iennarella-Servantez et al., 2021). These findings suggest that short-term feeding with a WD can induce a clinical response that mimics ***MetS*** in healthy dogs. The aim of this study was to characterize the metabolic and molecular signatures associated with a high-fat, high-monosaccharide, and low-fiber isocaloric WD after ten weeks in dogs. Once established, this preclinical model can be used to assess the therapeutic benefits of novel antidiabetic therapy in the context of obesity-independent ***MetS***, and pave the way for translational studies that could benefit both human and veterinary medicine.

METHODS

Animals

Experimental procedures were approved by the Institutional Animal Care and Use Committee at Iowa State University (Protocol Number: 21-164). All methods were performed in accordance with the relevant guidelines and regulations at Iowa State University. The authors complied with ARRIVE guidelines in the completion of this study.

The study population consisted of 18 neutered young adult Beagles (9 males and 9 females, age 23-26 months) weighing between 7.5 and 11.5 kg. Prior to inclusion, each dog was assessed for its general health and condition with a physical examination and had received appropriate vaccinations and deworming treatments. Normal cardiovascular structure and function were confirmed through an echocardiogram performed prior to acclimation to the study facility. No dog had received topical or systemic medications within the 28 days preceding inclusion.

Each animal was assigned a unique 4-letter ear tattoo for identification purposes. Throughout the in-life phase, daily evaluations of the animals' general health and behavior were conducted by the study veterinarian (Dr. Agnes Bourgois-Mochel). Body weight and body condition scores (recorded as “underweight” vs. “ideal” vs. “overweight”) were recorded on a weekly basis. All observations, including any adverse events and study interventions were systematically recorded in the raw data file.

Housing

The study animals were acclimatized to the facility for one week before the start of the study. Housing conditions were strictly in accordance with the requirements set by the United States Department of Agriculture. Each dog was housed in a 16-square foot kennel (dimensions: 4'x4') with an interconnecting door, allowing for the co-housing of two animals. However, individual separation was implemented during specific periods, such as feeding times, or when necessary for specific interventions or observations.

The lighting schedule was kept from 6 a.m. to 6 p.m. The ambient temperature within the housing facilities was consistently set to 70°F (21.1°C), with continuous monitoring.

Throughout the study, the recorded temperature varied minimally, with the range extending from 67°F (19.4°C) to 72°F (22.2°C).

Relative humidity was also closely monitored, with values fluctuating between 34% and 45%. The dogs were provided with unrestricted access to tap water, delivered via individual nipple water feeders.

Experimental Design

In order to replicate the dietary intake of an average American diet, dogs were fed a high-fat, high-monosaccharide, low-fiber WD adjusted from parameters of the National Health and Nutrition Examination Survey (NHANES 2015-2016: Males and Females over 20 years) for ten weeks. Dogs were fed isocalorically based on individually calculated metabolizable energy needs. Blood samples were collected at baseline (***BAS1***) when dogs were fed their regular diet, and then again after ten weeks of WD feeding (***BAS2***).

Diet Composition for *BAS1* Measurements

Dogs were fed a daily diet of Royal Canin® Beagle Adult dry food (12% fat content), once in the morning, around 9 a.m. The portion size for each dog was individually calculated based on weight and resting energy requirements. Any leftover food was weighed and recorded in the raw data file.

Diet Composition for *BAS2* Measurements

Western diets were formulated to model the average intake of American subjects over 20 years from the NHANES and were fed to meet the nutrient and energy requirements for each dog. Diets were home cooked and offered once daily in the morning, around 9 a.m. In cases where the provided meal was not entirely consumed, the remaining portion was carefully weighed and documented in the raw data file. The exact composition of the WD can be found in **Table 1**.

Sample Collection

- Blood samples were drawn using a jugular catheter whenever possible, or from the saphenous or cephalic veins with single use needles. Blood samples were collected at baseline (***BAS1***) when dogs were fed their regular diet, and then again after ten weeks of WD feeding (***BAS2***) for measurement of:

    - Complete blood count (CBC) (plasma, K3 EDTA, Iowa State University College of Veterinary Medicine);
    - Standard chemistry panel, including alanine aminotransferase (ALT), alkaline phosphatase (ALP), albumin, total protein, triglycerides, total cholesterol, blood urea nitrogen (BUN), serum creatinine, serum bicarbonates, calcium, phosphorus, chloride, sodium and potassium (serum, plain tube, Iowa State University College of Veterinary Medicine);
    - Fasting blood glucose (serum, plain tube, Iowa State University College of Veterinary Medicine);
    - Glucagon[1] and insulin[2] (serum, plain tube, Cornell University College of Veterinary Medicine);
    - Lipid profiling: High-Density Lipoprotein (HDL) and Low-Density Lipoprotein (LDL) cholesterol (serum, plain tube, Texas A&M College of Veterinary Medicine);
    - Renin-angiotensin aldosterone system (RAAS) biomarkers (serum, plain tube, Attoquant Diagnostics, Vienna);
    - N-terminal prohormone of brain natriuretic peptide (NT-proBNP[3]) (plasma, K3 EDTA, IDEXX Laboratories, Maine);
    - Oxidative stress biomarkers (serum, plain tube, University of Murcia Facultad de Veterinaria);

[1] EMD Millipore's Glucagon Radioimmunoassay (RIA) Kit GL-32K.

[2] EMD Millipore's Human Insulin Radioimmunoassay (RIA) Kit HI-14K.

[3] IDEXX Laboratories Cardiopet ProBNP Test-Canine.

    - Metabolomics, including (1) General Metabolism; (2) Complex Lipids and (3) Biogenic Amines (serum, plain tube, University of California Davis Genome Center).
- Voided urine and fecal samples were collected at ***BAS1*** and ***BAS2*** for the purpose of conducting metabolomic analyses, including (1) General Metabolism; (2) Complex Lipids and (3) Biogenic Amines (University of California Davis Genome Center).
- BP was measured at ***BAS1*** and ***BAS2*** by a certified cardiologist using a Doppler device, following standard procedures from the American College of Veterinary Internal Medicine (ACVIM), as outlined in consensus panel guidelines (Acierno et al., 2018). As Doppler-derived single measurements of blood pressure are an estimate of systolic blood pressure (SBP) (Littman, 1994), the abbreviation SBP will be used throughout this manuscript. To avoid any potential disruptions or bias in the recordings, these measurements were consistently taken before any blood was collected during each study period. To follow the consensus panel guidelines for assessing hypertension (Acierno et al., 2018) and ensure accuracy, five consecutive and consistent SBP measurements were obtained from each subject. These values were then averaged to calculate an individual estimate of SBP.

A comprehensive overview of the experimental procedure, including a visual timeline of the study with specific sampling days, is presented in **Figure 2**.

Specific Analytical Methods

<u>Lipoprotein Profiling</u>

Lipoprotein profiling was carried out using the continuous lipoprotein density profiling (CLPDP) method, adhering to procedures detailed in prior literature (Larner, 2012; Minamoto et al., 2018). Briefly, a solution of 0.18 M NaBiEDTA (Tokyo Chemical Industry) measuring 1280 µL was combined with 10 µL of both serum and NBD C6-ceramide (Cayman Chemical Company). Subsequently, 1150 µL of the resultant blend was allocated to a polycarbonate centrifuge container (Beckman Coulter). The samples underwent centrifugation for 6 hours at 4ºC and 867,747 *g* using an Optima MAX-LP

ultracentrifuge (Beckman Coulter) equipped with a fixed-angle rotor (MLA-130; Beckman Coulter). Immediately post-centrifugation, the samples were imaged using a fluorescence imaging system comprising a digital camera (Quantifire XI; Optronics) and a constant metal halide light source (Dolan-Jenner Industries).

The images obtained were transformed into density profiles via software analysis (OriginPro7.5; OriginLab). Lipoprotein profiles were produced by plotting the average intensity of fluorescence on the y-axis, while the actual centrifuge tube coordinates (mm) served as the x-axis. A unique numbering system was established for the statistical examination. The area under the curve (AUC) of the total fluorescence trace and each segment were used to determine the total lipoprotein intensity and fractional intensities, respectively. AUCs were then calculated for LDLs and HDLs based on their density intervals. Individual AUC values were finally normalized using the total AUC and expressed as percentage, as presented by Minamoto et al. (2018).

RAAS Fingerprinting

Determination of angiotensin and aldosterone analytes from canine serum was derived as previously published by our consortium (Ward et al., 2021; Ward et al., 2022; Sotillo et al., 2023; Schneider et al., 2023). Briefly, serum samples were analyzed to determine the equilibrium concentrations of Angiotensin I (Ang I (1–10)), Angiotensin II (Ang II (1–8)), Angiotensin III (Ang III (2–8)), Angiotensin IV (Ang IV (3–8)), Angiotensin 1–7 (Ang1–7), Angiotensin 1–5 (Ang1–5), and aldosterone using validated Liquid Chromatography-Tandem Mass Spectrometry (LC-MS/MS) assays at a commercial laboratory[4] (Domenig et al., 2016). Following *ex vivo* equilibration, each sample was spiked with a stable isotope-labeled internal standard for each angiotensin peptide and a deuterated internal standard for aldosterone (aldosterone D4). The analytes were then extracted using C18-based solid-phase extraction. The extracted samples underwent mass spectrometry analysis using a reversed-analytical column, which was operated in tandem with a XEVO TQ-S triple quadrupole mass spectrometer in multiple reaction monitoring mode.

[4] Attoquant Diagnostics, Vienna, Austria.

Internal standards were used to ensure analyte recovery throughout the sample preparation process for each sample. Concentrations of the analytes were calculated from the integrated chromatograms when the integrated signals exceeded a signal-to-noise ratio of 10, taking into account the corresponding response factors derived from suitable calibration curves in the serum matrix. The lower limit of quantification (LLOQ) was established at 3.0 pM, 2.0 pM, 3.0 pM, 2.0 pM, 2.5 pM, 2.0 pM and 13.9 pM for Ang I (1–10)), Ang II (1–8), Ang1–7, Ang1–5, Ang III (2–8), Ang IV (3–8) and aldosterone, respectively.

Markers for renin (PRA–S) and angiotensin-converting enzyme (ACE–S) based on angiotensin were obtained from Ang II (1–8) and Ang I (1–10) levels by calculating their sum and ratio, respectively (Guo et al., 2020). Renin-independent alternative RAAS activation (ALT–S) was calculated using the formula [(Ang 1-7 + Ang 1-5) / (Ang I + Ang II + Ang 1-7 + Ang 1-5)] (Zoufaly et al., 2020).

Oxidative Stress Markers

The development and validation of analytical techniques for assessing oxidative stress markers adhered to protocols outlined in previous studies (González-Arostegui et al., 2022). The following provides an abridged overview of the specific procedures used in evaluating antioxidant and oxidant statuses.

Antioxidant Status

- The *Cupric Reducing Antioxidant Capacity* (**CUPRAC**) assay, initially described by Campos et al. (2009), is based on the conversion of Cu^{2+} to Cu^{+} through the action of non-enzymatic antioxidants in the serum sample. Quantification of CUPRAC followed the protocol previously validated for canine serum (Rubio et al., 2016), with results reported in mmol/L.
- The *Ferric Reducing Ability of Plasma* (**FRAP**) assay relies on the conversion of ferric-tripyridyltriazine (Fe^{3+}-TPTZ) to its ferrous form (Benzie et al., 1996). Quantification of FRAP was performed as described in previous studies (Benzie et al., 1996; Rubio et al., 2017). Results are expressed in mmol/L.

- Measurements of *Trolox Equivalent Antioxidant Capacity* (**TEAC**) followed the procedures outlined by Arnao et al. (1996) later adapted to canine serum samples by Rubio et al. (2016). The assay involves the generation of ABTS radicals and their subsequent reduction by non-enzymatic antioxidants in the serum specimen (Arnao et al., 1996), with results presented in mmol/L.
- **Total thiol** (µmol/L) determination was based on the reaction between sample thiols and DTNB (Jocelyn, 1987; Da Costa et al., 2006).
- The evaluation of *Paraoxonase type 1* (**PON-1**) was based on the conversion of phenylacetate to phenol, following the same methods used for canine serum by Tvarijonaviciute et al. (2012a). Results are expressed as IU/mL.
- Quantification of *Glutathione Peroxidase* (**GPx**) activity was performed using a commercial assay kit according to the manufacturer's instructions[5], as described in previous studies (Kapun et al., 2012; Verk et al., 2017). Results are reported in IU/ml units.

Oxidant Status

- The *Total Oxidant Status* (**TOS**) was determined following Erel's method (2005), which had previously been applied to dog serum (Rubio et al., 2016). Results are expressed in µmol/L.
- The *Peroxide-Activity* (**POX-Act**) assay involved the detection of total peroxides through a peroxide-peroxidase reaction using tetramethylbenzidine as the chromogenic substrate (Tatzber et al., 2003). Results are expressed in µmol/L.
- The *Derivatives-Reactive Oxygen Metabolites* (**d-ROMs**) assay used an acidic medium to react with the sample in the presence of DEPPD, as per the method previously established by Alberti et al. (2000). Results are reported in Carratelli Units (U.CARR).
- Determination of *Advanced Oxidation Protein Products* (**AOPP**) was based on oxidized albumin and di-tyrosine containing cross-linked proteins, as described in

[5] RANDOX Glutathione Peroxidase (Ransel) Kit RS504

previous studies (Witko-Sarsat et al., 1996; Rubio et al., 2018). Results are expressed in µmol/L.

Serum/Urine/Fecal Metabolomics

General Metabolism

Samples were extracted using the extraction procedure by Matyash et al. (2008), which includes MTBE, MeOH, and H_2O. The organic (upper) phase was dried down and submitted for resuspension and injection onto the LC, while the aqueous (bottom) phase was dried down and submitted for derivatization for GC. Samples were shaken at 30°C for 1.5 hours. Then, 91 µL of MSTFA + FAMEs were added to each sample, and tubes were shaken at 37°C for 0.5 hours to complete the derivatization. Samples were then vialed, capped, and injected onto the instrument. A 7890A GC coupled with a LECO time of flight mass spectrometer (TOFMS) was used for the procedure. Then, 0.5 µL of the derivatized sample was injected using a splitless method onto a RESTEK RTX-5SIL MS column (30 m × 0.25 mm inner diameter with 0.25 µm film thickness) with an Intergra-Guard at 275°C with a helium flow of 1 mL/min. The GC oven was set to hold at 50°C for 1 minute, then ramped up to 20°C/min to 330°C and held for 5 minutes. The transfer line was set to 280°C, while the EI ion source was set to 250°C. The mass spectrometry parameters collected data from 85 m/z to 500 m/z at an acquisition rate of 17 spectra/second. All compounds detected were tentatively identified to the Metabolomics Standards Initiative (MSI) Level 2 with a spectral library match score of 800 or higher (Sumner et al., 2007).

Complex Lipids

Samples were extracted using the extraction procedure by Matyash et al. (2008), which includes MTBE, MeOH, and H_2O. The organic (upper) phase was dried down and resuspended for injection onto the LC, while the aqueous (bottom) phase was dried down and submitted for derivatization for GC. The samples were then resuspended with 110 µL of a solution of 9:1 methanol:toluene and 50 ng/mL CUDA. Samples were then shaken

for 20 seconds, sonicated for 5 minutes at room temperature, and centrifuged for 2 minutes at 16100 rcf. Thirty three µL of samples were aliquoted into a vial with a 50 µL glass insert for positive and negative mode lipidomics. The samples were then loaded onto an Agilent 1290 Infinity LC stack. The positive mode was run on an Agilent 6546 with a scan range of m/z 120-1200 Da and an acquisition speed of 2 spectra/s. Positive mode had between 0.5 and 2 µL injected onto an Acquity Premier BEH C18 1.7 µm, 2.1 x 50 mm column. The gradient used was 0 min 15% (B), 0.75 min 30% (B), 0.98 min 48% (B), 4.00 min 82% (B), 4.13-4.50 min 99% (B), 4.58-5.50 min 15% (B) with a flow rate of 0.8 mL/min. Another aliquot was run in negative mode on an Agilent 1290 Infinity LC stack and injected onto the same column, with the same gradient, using an Agilent 6550 QTOF mass spectrometer. The acquisition rate was two spectra per second with a scan range of m/z 60-1200 Da. The mass resolution for the Agilent 6530 is 10,000 for ESI (+) and 20,000 for ESI (-) for the Agilent 6550.

Biogenic Amines

Sample extraction for biogenic amines consisted of a liquid-liquid extraction method (Matyash et al., 2008) with MTBE, methanol, and water, creating a biphasic partition. The polar phase was then dried down to completion and run on a Waters Premier Acquity BEH Amide column. A short 4-minute liquid chromatography method was used for the separation of polar metabolites from a starting condition of 100% LCMS H_2O with 10 mM ammonium formate and 0.125% formic acid to an end condition of 100% ACN:H_2O 95:5 (v/v) with 10 mM ammonium formate and 0.125% formic acid. A Sciex Triple-ToF scanned from 50-1500 m/z with MS/MS collection from 40-1000, selecting the top five ions per cycle. Data processing was done with MS-Dial using an MZ-RT list for annotations, in addition to a library for MS/MS matching.

Statistics

The sample size for this experiment was established based on preliminary data from a previous study conducted by our group (Iennarella et al., 2021). In that study, statistically significant differences in BP and total cholesterol were observed in a group of ten dogs receiving an isocaloric WD, with an alpha level of 0.05 and a statistical power of 80%.

Study variables were visually inspected for normality, summarized, and displayed as median (interquartile range [IQR]). Differences between ***BAS1*** and ***BAS2*** were analyzed using non-parametric Wilcoxon signed rank test with continuity correction. *P*-values < 0.05 were considered statistically significant. The R[6] software version 4.2.2 was used for statistical analyses. (R Core Team (2022). Graphical representation of the data was produced using the *ggplot2* package in R version 4.2.2.

For metabolomic analyses, the peak tables were uploaded into the Matlab® (R2023b, The Mathworks Inc., Natick, MA) environment and converted to datasets with appropriate class labels. In PLS_Toolbox (Version 9.0; Eigenvector Research, Manson, WA), Principal Component Analysis (PCA) was performed on the autoscaled data. To determine the variables responsible for differences between groups, Cluster Resolution Feature Selection (FS-CR) was applied (Sinkov et al., 2011; Adutwum et al., 2017). For each dataset, the FS-CR process of sequential backward elimination and forward selection was repeated 100 times, permuting the subsets of data, and only variables selected 85% of the time were retained to prevent overfitting (Sinkov et al., 2011). The distance between clusters (cluster resolution) was used to determine which variables contributed to the separation between classes (Sinkov et al., 2011). PCA was then performed using the selected variables from FS-CR, and the variables and their loadings were extracted.

[6] R: A language and environment for statistical computing. R Foundation for Statistical Computing, Vienna, Austria. URL https://www.R-project.org/).

RESULTS

Physical Examination and Adverse Events

The study veterinarian, along with approved study personnel, conducted weekly physical examinations and reported no notable changes in the dogs' overall condition, behavior, cardiovascular system, hydration level, respiratory system, or skin appearance throughout the study.

During the transition from their regular diet (Royal Canin® Beagle Adult) in the first baseline phase (***BAS1***) to the Western diet (***BAS2***), several dogs experienced one or more episodes of softened stools. These instances were considered as "non-serious" digestive adverse events by the study veterinarian and resolved on their own within a few days. No significant adverse effects were reported over the duration of the study.

Body Weight

Differences in body weight between ***BAS1*** (8.9 [7.8 to 9.6] kg) and ***BAS2*** (8.7 [7.4 to 9.2] kg) were statistically significant ($P < 0.001$), but were not considered clinically meaningful by the study veterinarian. Overall, no changes of more than (-) 13% in individual weights from ***BAS1*** to ***BAS2*** were reported after ten weeks of feeding with the WD. Similarly, no notable changes in body condition scores were reported between ***BAS1*** (N = 0, 13 and 5 for “underweight”, “ideal” and “overweight”, respectively) and ***BAS2*** (N = 1, 11 and 6 for “underweight”, “ideal” and “overweight”, respectively).

Complete Blood Count and Chemistry

All hematological parameters were within normal physiological limits, and there were no clinically relevant or statistically significant changes in CBC between ***BAS1*** and ***BAS2***.

No significant changes in liver-related chemical parameters, including ALT, ALP, albumin, and total protein, were observed between ***BAS1*** and ***BAS2***. However, dogs fed a WD for ten weeks had a decrease in serum bicarbonate (-2.5 [-4.0 to -1.0] mEq/L, $P < 0.001$), phosphorus (-0.8 [-1.3 to -0.5] mg/dL, $P < 0.001$), and potassium (-0.5 [-0.7 to -0.3] mEq/L,

$P < 0.001$), and an increase in chloride levels (+1.5 [0.0 to 3.0] mEq/L, $P = 0.001$). The diet also induced some borderline statistically significant changes in calcium ($P = 0.049$) and sodium ($P = 0.041$) levels at ***BAS2***. Additionally, there was a significant decrease in BUN at ***BAS2*** (-4.5 [-5.0 to -3.0] mg/dL, $P < 0.001$), along with an increase in serum creatinine (+0.1 [0.0 to 0.2] mg/dL, $P = 0.001$). These variations, although statistically significant, remained within physiological limits. A summary of the clinical chemistry parameters at ***BAS1*** and ***BAS2*** is presented in **Figure 3**.

Fasting Blood Glucose, Serum Insulin and Glucagon

The biological effects of the WD on fasting blood glucose, as well as the glucose-regulating hormones insulin and glucagon, are presented in **Figure 4**. Over a span of ten weeks, the WD induced a significant increase in fasting blood glucose concentrations. This increase approached the upper physiological limit, demonstrating an average increase of 15.8% relative to baseline (***BAS1*** 88.0 [82.0 to 91.0] mg/dL vs. ***BAS2*** 102.5 [95.0 to 109.0] mg/dL, $P < 0.001$).

The increase in fasting blood glucose was accompanied by a significant decrease of 25.6% in circulating insulin concentrations (***BAS1*** 11.6 [10.2 to 12.3] uIU/mL vs. ***BAS2*** 7.4 [5.2 to 10.4] uIU/mL, $P = 0.04$). Furthermore, a trend indicative of a decline in serum glucagon concentrations was observed at ***BAS2*** (***BAS1*** 69.3 [64.0 to 77.2] pg/mL vs. ***BAS2*** 61.8 [49.8 to 64.3] pg/mL); however, it did not reach statistical significance ($P = 0.055$).

Blood Pressure

Overall, SBP measurements were significantly higher at ***BAS2*** compared with pre-WD readings (***BAS1*** 133.5 [126.0 to 141.0] mmHg vs. ***BAS2*** 143.0 [133.0 to 152.0] mmHg, $P = 0.017$) (**Figure 5**).

Renin-Angiotensin System (RAAS)

Our analysis revealed a slight downward trend in biomarkers in both the traditional and alternative arms of the RAAS, though this trend was not statistically significant. This included reductions in plasma renin activity (PRA–S), Angiotensin I (Ang I (1–10)), Angiotensin II (Ang II (1–8)), Angiotensin III (Ang III (2–8)), Angiotensin IV (Ang IV (3–8)), Angiotensin 1–7 (Ang1–7), and Angiotensin 1–5 (Ang1–5).

A comprehensive overview of the RAAS biomarker profile is provided in **Table 2**. Importantly, aldosterone data was not available for statistical analysis, as over 45% of the samples had analyte levels below the lower limit of quantification.

Total Cholesterol, Triglycerides and Lipoproteins

Figure 6 summarizes the impact of the WD on total cholesterol, HDL-cholesterol and LDL-cholesterol levels. After ten weeks of feeding with the WD, there was a 44.0% increase in total cholesterol levels (from ***BAS1*** 130.0 [125.0 to 145.0] mg/dL to ***BAS2*** 187.5 [173.0 to 219.0] mg/dL, $P < 0.001$), along with a significant reduction in HDL-cholesterol (from ***BAS1*** 84.2 [80.5 to 85.6] % to ***BAS2*** 81.1 [72.8 to 83.1] %, $P < 0.001$) and a 26.8% elevation in LDL-cholesterol (from ***BAS1*** 14.5 [13.0 to 17.0] % to ***BAS2*** 18.0 [15.5 to 24.5] %, $P < 0.001$). The detailed lipoprotein profiles, including levels at both baseline (***BAS1)*** and post-WD feeding (***BAS2***), along with their statistical significance, are presented in **Table 3**. Notably, these changes were not accompanied by significant alterations in serum triglyceride levels ($P = 0.54$).

NT-proBNP

The levels of NT-proBNP significantly increased after the WD, as shown by the change from baseline (***BAS***1 250.0 [250.0 to 401.0] pmol/L) to post-WD (***BAS2*** 460.5 [330.0 to 750.0] pmol/L) ($P < 0.001$). Notably, two dogs exhibited NT-proBNP concentrations exceeding 900 pmol/L.

Oxidative Stress

Antioxidant Status

Overall, the effect of the WD on antioxidant markers was mild, with no significant changes in CUPRAC, FRAP, TEAC, and Thiol values. In contrast, PON-1 levels significantly decreased at ***BAS2*** compared to ***BAS1*** (***BAS1*** 4.2 [3.7 to 4.4] IU/mL vs. ***BAS2*** 3.8 [3.6 to 4.0] IU/mL, $P = 0.004$), and GPx activity increased significantly at ***BAS2*** (***BAS1*** 6460.0 [5448.0 to 7764.0] U/L vs. ***BAS2*** 8432.0 [6964.0 to 8852.0] U/L, $P < 0.001$). These effects are summarized in **Figure 7(A)**.

Oxidant Status

The impact of the WD on oxidative stress parameters was more consistent, with total oxidant status significantly increasing at ***BAS2*** (***BAS1*** 4.8 [3.9 to 5.8] µmol/L vs. ***BAS2*** 7.0 [4.9 to 8.7] µmol/L, $P = 0.018$). The increase extended to reactive oxygen metabolites (***BAS1*** 21.3 [13.2 to 28.9] U.CARR vs. ***BAS2*** 28.8 [17.9 to 43.0] U.CARR, $P = 0.084$). Conversely, there was a decrease in POX-Act post-WD (***BAS1*** 101.8 [79.1 to 114.0] µmol/L vs. ***BAS2*** 92.3 [62.1 to 94.2] µmol/L, $P < 0.001$). However, there were no discernible effects on AOPP (**Figure 7(B)**).

Metabolomics

General Metabolism

Before feature selection, a clear separation between ***BAS1*** and ***BAS2*** was observed in the PCAs for urine, stool, and serum (**Figure 8**). To identify variables responsible for this separation, FS-CR was further employed (Sinkov et al., 2011; Armstrong et al., 2021; Adutwum et al., 2017). FS-CR identified 48 significant metabolites in the urine samples, 37 significant metabolites in stool samples, and 10 in serum samples. The loadings of the selected variables are included in the **Supplementary Information** (**Supplementary Figures 1-3, 2-6 and 7-9**, for *General Metabolism*, *Complex Lipids* and *Biogenic Amines*, respectively). Following feature selection, ***BAS1*** and ***BAS2*** were clearly separated along

PC1 for all three sample types, which explained 29.4%, 48.6%, and 82.3% of the total variance for urine, stool, and serum samples, respectively (**Figure 9**).

In urine, 29 metabolites were correlated with ***BAS1***, including pipecolinic acid, piperidone, cytosine, and nicotinamide (**Supplementary Table 1**). Additionally, 19 metabolites were strongly correlated with ***BAS2***, including 2,3-dihydroxybutanoic acid (tartaric acid), arabitol, cellobiose, and glycerol (**Supplementary Table 1**).

In stool, seven metabolites were correlated with ***BAS1***, such as cadaverine, trans-4-hydroxyproline, tryptamine, and isopalmitic acid (**Supplementary Table 2**). Thirty metabolites were strongly correlated to ***BAS2***, including fructose, pipecolinic acid, erythrose, and 2-deoxyerythritol (**Supplementary Table 2**).

In serum, nine of the ten significant metabolites from FS-CR were correlated to ***BAS1***, including 3-Amino-2-piperidone and 2-picolinic acid (**Supplementary Table 3**).

Complex Lipids

Prior to feature selection, no separation was observed between ***BAS1*** and ***BAS2*** for complex lipid urine samples (**Figure 10(A)**). However, separation between ***BAS1*** and ***BAS2*** was observed along PC1 and PC2 for stool (**Figure 10(B)**), and along PC1 for serum (**Figure 10(C)**).

With feature selection, a clear separation was achieved between ***BAS1*** and ***BAS2*** along PC1 for all three biospecimens (**Figure 11**). It is noteworthy that more than three-quarters of the total variation was explained by PC1 for stool (76.7%) and serum (82.6%) samples. With FS-CR, 36 lipids in urine, 36 in stool, and 30 in serum were selected as significant metabolites describing differences between ***BAS1*** and ***BAS2***.

In urine, 25 lipids were correlated with ***BAS1*** and 11 lipids were correlated with ***BAS2*** (**Supplementary Table 4**).

In stool, 32 lipids were correlated with ***BAS1***, including eicosapentaenoic acid and various triglycerides, and four lipids were correlated with ***BAS2***, including margaric acid (**Supplementary Table 5**).

In serum, 14 lipids were correlated with ***BAS1***, including phosphatidylcholine 38:5 and phosphatidylcholine 40:7, and 16 lipids were correlated with BAS2, including sphingomyelin (d36:2) and a number of phosphatidylcholines (**Supplementary Table 6**).

Biogenic Amines

Prior to feature selection, there was significant overlap between ***BAS1*** and ***BAS2*** for urine (**Figure 12(A)**). However, for stool (17.6%) and serum (11.8%) samples, there was a clear separation along PC2 (**Figure 12(B) and (C)**). FS-CR identified 90 significant metabolites in urine, 68 significant metabolites in stool, and 26 significant metabolites in serum. After feature selection, ***BAS1*** and ***BAS2*** samples were clearly separated along PC1 for all biospecimens, accounting for approximately half of the total variance in the experimental data (**Figure 13**).

In urine, 47 metabolites were correlated with ***BAS1***, including N-acetylmannosamine, threonic acid, nicotinamide, and dopamine (**Supplementary Table 7**). Additionally, 43 urinary metabolites correlated with ***BAS2***, including N-methylphenylalanine, tartaric acid, and propoxyphene (**Supplementary Table 7**).

In stool, 51 metabolites were correlated with ***BAS1***, including O-acetylsalicylic acid, caffeic acid, and 3-pyridinemethanol, while 17 metabolites were correlated with ***BAS2***, including stachydrine and prochlorperazine (**Supplementary Table 8**).

In serum, 11 metabolites were correlated with ***BAS1***, including 4-aminobenzoic acid and L-histidinol, while 15 metabolites were correlated with ***BAS2***, including secnidazole, tartaric acid, and vanillin (**Supplementary Table 9**).

DISCUSSION

Several landmark trials have demonstrated the efficacy of SGLT-2 inhibitors and GLP-1 receptor agonists in managing T2DM, with benefits extending to cardiovascular diseases and renal protection (Zinman et al., 2015; Neal et al., 2017; Birkeland et al., 2017; Persson et al., 2018; Perkovic et al., 2019; Inzucchi et al., 2020; Packer et al., 2020; Kosiborod et al., 2023). These findings provide further evidence of the multifaceted benefits of these therapeutic drugs beyond glycemic control. The pleiotropic effects of SGLT-2 inhibitors and GLP-1 agonists hold the potential to target cardiorenal, hepatic and metabolic disorders using a disease model that replicates key features of ***MetS***. Previous studies have primarily focused on obesity-related metabolic dysfunction when examining the effects of WDs in dogs. However, there is a lack of comprehensive studies on the biological and metabolic impacts of WDs independent of obesity. This is relevant as most clinical investigations on the effectiveness of dapagliflozin and empagliflozin for cardiovascular and renal outcomes had a majority of non-obese subjects (McMurray et al., 2019; Wheeler et al. 2020; Butler et al., 2021; Oyama et al., 2022; EMPA-KIDNEY Collaborative Group, 2023). Furthermore, a recent study by Adamson et al. (2021) confirms that the effectiveness of dapagliflozin in treating heart failure patients with reduced ejection fraction remains consistent regardless of their body mass index. Collectively, these findings provide a strong rationale for studying the pharmacodynamic effects of novel antidiabetic therapy in a metabolic dysfunction model that is not dependent on obesity.

Our study maintained isocaloric conditions to isolate the effect of the diet's composition from obesity as a confounding factor. It builds on preliminary data from Lyu et al. (2022), which showed a tendency towards elevated glucose levels in ten healthy Beagles under an isocaloric high-fat diet for six weeks. To the best of our knowledge, our research represents the first comprehensive characterization of the biological effects of a WD model, independent of obesity. By inducing ***MetS*** without causing weight gain, we have successfully developed a non-invasive, inducible, and potentially reversible preclinical model in just a few weeks. For ethical reasons and considerations related to animal welfare, it is important to emphasize that our objective was *not* to induce clinical symptoms of ***MetS*** in our study. Therefore, the majority of the observed changes reported

herein remained within physiological limits. Overall, the WD was well tolerated, with no adverse events reported during the course of the study. Minor digestive issues appeared when transitioning from a regular diet to the WD, but they resolved within a few days.

Hematological parameters consistently remained within normal physiological limits, showing no clinically meaningful changes. The most notable variations were observed in metabolic parameters. Specifically, the WD induced a statistically significant increase in fasting blood glucose levels, nearing the upper physiological limit. This resulted in an average increase of approximately 20% in blood glucose concentrations compared to baseline. Interestingly, this observation was accompanied by a significant decrease (around 30%) in circulating insulin levels, which could indicate impaired insulin secretion, as seen in T2DM (Clark et al., 2001). It is worth noting that our results differ from previous findings where plasma insulin levels increased in cases related to obesity-related metabolic dysfunction in dogs (Tvarijonaviciute et al., 2012b; Moinard et al., 2020). This highlights the value of our approach in modeling key features of ***MetS*** pathophysiology independently of obesity. The decrease in circulating glucagon levels may be indicative of a physiological feedback mechanism in order to maintain glucose homeostasis in response to increased FBG and reduced insulin concentrations (Rix et al., 2019).

Our dietary intervention also resulted in significant changes to serum chemistry parameters. These fluctuations, although still within physiological limits, demonstrate the ability of our model to greatly influence metabolism and homeostasis. Specifically, we observed a decrease in serum bicarbonate levels, which is in line with low-grade metabolic acidosis (Burger and Schaller, 2023). This is important because a recent meta-analysis, which included data from over 30,000 patients, found an association between ***MetS***, lower bicarbonate levels, and a higher risk of metabolic acidosis (Lambert et al., 2023). Concurrently, there was a measurable increase in chloride levels, which may be attributed to hyperchloremic acidosis (Sharma et al., 2023) and/or the onset of ***MetS*** (Kimura et al., 2016). In addition, the WD induced marked reductions in both phosphorus and potassium levels, both of which have been linked to an increased risk for ***MetS*** (Kalaitzidis et al., 2005; Stoian and Stoica, 2014; Sun et al., 2014).

Consistent with the definition of ***MetS*** by the National Heart, Lung, and Blood Institute (NHLBI), our diet induced a significant elevation of SBP by approximately 10 mmHg. Interestingly, SBP was not found to increase in a previous canine study focusing on obesity-related cardiac dysfunction and ***MetS*** (Tropf et al., 2017), again supporting our rationale for studying the effect of western diets independently of obesity. Our study also found mild increases in NTproBNP, although mostly within the reference range. We suspect that the increase in circulating natriuretic peptides occurred secondarily to the increase in SBP, as previously reported in the literature (Hussain et al., 2022; Jang et al., 2023), but it could also be indicative of cardiac stress (Bayes-Genis et al., 2023). Notably, some dogs showed NT-proBNP concentrations exceeding 900 pmol/L, a level commonly associated with structural heart disease in canines (Singletary et al., 2012; Wilshaw et al., 2021).

Total cholesterol increased by approximately 45% after ten weeks. Importantly, in line with the definition of ***MetS***, dogs fed the isocaloric WD model experienced a significant reduction in HDL-cholesterol, along with an increase of LDL-cholesterol (of around 25%). These shifts occurred independently of any corresponding alterations in serum triglyceride levels. While surprising, this finding is consistent with earlier research from Lahm Cardoso et al. (2016) which showed a strong correlation between body condition scores (BCS) and triglyceride levels in dogs, with values approaching the upper limit of 200 mg/dL in dogs with a BCS of 8 or above (classified as "overweight" or "obese" in our study).

Our results on redox status align with previous human studies (Matsuzawa-Nagata et al., 2008; Boden et al., 2017; Aleksandrova et al., 2021). Specifically, we observed significant increases in TOS and d-ROMs at ***BAS2***. In contrast, the effect on antioxidant markers was more nuanced and generally mild, with levels of CUPRAC, FRAP, TEAC, and Thiol remaining stable at ***BAS2***. This is in line with the variable impact of dietary fat on systemic antioxidative stress markers in dogs. Some studies have shown no effect of carbohydrate and fat concentrations on oxidative stress biomarkers (Chiofalo et al., 2020), while others have reported an increase in antioxidant capacity, but no effect on oxidative stress markers (Vecchiato et al., 2023).

Our study highlights the comprehensive metabolic changes induced by the WD, which impacts various biological pathways, including those related to general metabolism, complex lipids, and biogenic amines. These observations underscore the potential relevance of this model in studying ***MetS*** and its associated health complications. Notably, all the metabolites detected in our study were classified according to MSI Level 2 standards (Sumner et al., 2007). The correlation of nicotinamide to the baseline diet (***BAS1***) in both general metabolism (urine) and biogenic amines (urine) suggests that dogs had lower levels of this essential form of vitamin B3 after ten weeks of feeding with a WD (***BAS2***) compared to their standard diet. Nicotinamide plays a crucial role in various metabolic pathways, particularly in energy production and DNA repair (Surjana et al., 2010; Amjad et al., 2021). Similarly, the correlation of glycerol to ***BAS2*** in general metabolomics (urine) indicates that glycerol levels were increased during feeding with the WD. Glycerol is a key component of triglycerides and is involved in energy metabolism, especially in lipid breakdown and synthesis (Frühbeck et al., 2014). This elevation is likely related to an increased metabolism of triglycerides caused by the WD, indicating a potential shift in lipid metabolism. The correlation of tartaric acid (2,3-dihydrobutanoic acid) with ***BAS2*** in multiple classes (general metabolomics in urine, biogenic amines in urine, and biogenic amines in serum) indicates that tartaric acid levels increased during the WD phase. These changes are likely associated with the increased catabolism of the antioxidant ascorbic acid and accompany variations in oxidative stress markers highlighted above (Bánhegyi et al., 2004).

A greater diversity of fatty acids was correlated with ***BAS1***, especially in stool, indicating a wider range of fatty acid profiles in the baseline diet. This diversity is essential for energy production and cell membrane structure (Hishikawa et al., 2014). Moreover, after the WD diet, saturated fatty acids (namely FA 17:0 in stool lipidomics and PC 18:0) were increased. High levels of saturated fatty acids have been linked to negative health outcomes such as cardiovascular diseases (Siri-Tarino et al., 2010; Hooper et al., 2020). The identified correlations between fatty acid diversity and saturated fatty acids suggest a significant change in lipid metabolism, a key feature of ***MetS***.

Palmitoleic acid, an omega-7 monounsaturated fatty acid commonly found in adipose tissues, was correlated with ***BAS2*** in stool general metabolomics. This increase may indicate alterations in adipose tissue metabolism, potentially related to the storage and release of lipids in response to the WD. Palmitoleic acid (16:1n7) increases lipolysis, glucose uptake and glucose utilization for energy production in white adipose cells (Bolsoni-Lopes et al., 2014; Cruz et al., 2018). Pipecolinic acid (found in urine general metabolomics) and 2-picolinic acid (found in serum general metabolomics) showed a correlation with ***BAS1***. These metabolites are byproducts of tryptophan metabolism. Tryptophan metabolism has been implicated in various physiological processes, such as neurotransmitter synthesis and immune regulation (Florensa-Zanuy et al., 2021).

In both general metabolomics (GC-MS) and LC-MS assays, several unidentified metabolites were detected. For GC-MS, this was due to spectral library matches failing to identify metabolites below the 800 threshold. Advanced data processing techniques, such as Parallel Factor Analysis, could be employed to deconvolve data and obtain cleaner spectra (Amigo et al., 2008; Giebelhaus et al., 2022a). However, this would require a separate and dedicated study. Additionally, the bioamines assay detected several non-amine compounds due to its ability to detect compounds without an amine group. With LC-MS, the presence of unidentified metabolites could possibly be attributed to biotransformation of known metabolites, which involves the addition or removal of specific chemical moieties such as (de)-glycosylation, (de)-methylation, (de)-amination, and (de)-hydroxylation. These transformations often occur during metabolic processes (Giebelhaus et al., 2022b). To identify these metabolites, biotransformation analysis techniques and exploration of additional libraries and databases would be necessary. However, this is beyond the scope of this study.

This study presents several limitations worth mentioning. First, the study was limited in size and did not address the potential for reversibility of the model, specifically regarding the metabolic impacts of transitioning back to a standard diet. While the non-invasive nature of the model suggests reversibility, this would need to be confirmed in a separate experiment. Additionally, the study lacks some functional data, such as the time-dependent effects of the WD on glucose and insulin levels, as well as intestinal

permeability and fecal microbiome composition. This was partly deliberate, as those effects have been extensively characterized previously in the literature (e.g., Moinard et al., 2020). Lastly, our diet failed to induce an increase in triglyceride levels, which is an important component of ***MetS***. This outcome was expected, however, given the isocaloric nature of the feeding regimen and existing literature that established a clear relationship between BCS and triglyceride levels in dogs (Lahm Cardoso et al., 2016).

In summary, our isocaloric WD, designed to mimic the NHANES diet, which is high in fat, monosaccharides, and low in fiber, effectively replicated key characteristics of ***MetS***. These included elevated BP, increased fasting glucose levels, and reduced HDL-cholesterol, all independent of abdominal obesity. Additionally, the WD induced significant changes in general metabolism, complex lipids, and biogenic amines in dogs, while also leading to a mild state of metabolic acidosis and elevated natriuretic peptides.
Our findings underscore the utility of this model for investigating the metabolic effects of novel antidiabetic therapies within the context of obesity-independent ***MetS***. Furthermore, this research opens the door to translational studies with potential benefits for both human and veterinary medicine.

BULLET POINT SUMMARY

What is already known?

- The pleiotropic effects of novel antidiabetic therapy provide an opportunity to impact cardiovascular-kidney-metabolic health.
- The effectiveness of dapagliflozin in heart failure is independent of the patient's body mass index.

What this study adds?

- This study establishes a non-invasive and inducible preclinical model of obesity-independent metabolic syndrome (***MetS***).
- First description of the metabolic signatures associated with Western diets independent of obesity.

Clinical significance?

- The canine model can be used to study the pharmacodynamics of antidiabetics in obesity-independent ***MetS***.
- This opens the door to translational studies with potential benefits for human and veterinary medicine.

REFERENCES

Acierno MJ, Brown S, Coleman AE, Jepson RE, Papich M, Stepien RL, Syme HM. ACVIM consensus statement: Guidelines for the identification, evaluation, and management of systemic hypertension in dogs and cats. J Vet Intern Med. 2018 Nov;32(6):1803-1822. doi: 10.1111/jvim.15331. Epub 2018 Oct 24. PMID: 30353952; PMCID: PMC6271319.

Adamson C, Jhund PS, Docherty KF, Bělohlávek J, Chiang CE, Diez M, Drożdż J, Dukát A, Howlett J, Ljungman CEA, Petrie MC, Schou M, Inzucchi SE, Køber L, Kosiborod MN, Martinez FA, Ponikowski P, Sabatine MS, Solomon SD, Bengtsson O, Langkilde AM, Lindholm D, Sjöstrand M, McMurray JJV. Efficacy of dapagliflozin in heart failure with reduced ejection fraction according to body mass index. Eur J Heart Fail. 2021 Oct;23(10):1662-1672. doi: 10.1002/ejhf.2308. Epub 2021 Jul 29. PMID: 34272791; PMCID: PMC9292627.

Adutwum LA, de la Mata AP, Bean HD, Hill JE, Harynuk JJ. Estimation of start and stop numbers for cluster resolution feature selection algorithm: an empirical approach using null distribution analysis of Fisher ratios. Anal Bioanal Chem. 2017 Nov;409(28):6699-6708. doi: 10.1007/s00216-017-0628-8. Epub 2017 Sep 29. PMID: 28963623; PMCID: PMC9677961.

Alberti A, Bolognini L, Macciantelli D, Caratelli M. The radical cation of N,N-diethyl-para-phenylendiamine: A possible indicator of oxidative stress in biological samples. Res. Chem. Intermed. 2000;26:253–267. doi: 10.1163/156856700X00769.

Aleksandrova K, Koelman L, Rodrigues CE. Dietary patterns and biomarkers of oxidative stress and inflammation: A systematic review of observational and intervention studies. Redox Biol. 2021 Jun;42:101869. doi: 10.1016/j.redox.2021.101869. Epub 2021 Jan 22. PMID: 33541846; PMCID: PMC8113044.

Amigo JM, Skov T, Bro R, Coello J, Maspoch S. Solving GC-MS problems with PARAFAC2. TrAC Trends in Analytical Chemistry 27:714–725. doi: 10.1016/j.trac.2008.05.011.

Amjad S, Nisar S, Bhat AA, Shah AR, Frenneaux MP, Fakhro K, Haris M, Reddy R, Patay Z, Baur J, Bagga P. Role of NAD^+ in regulating cellular and metabolic signaling pathways. Mol Metab. 2021 Jul;49:101195. doi: 10.1016/j.molmet.2021.101195. Epub 2021 Feb 17. PMID: 33609766; PMCID: PMC7973386.

Arnao MB, Cano A, Hernández-Ruiz J, García-Cánovas F, Acosta M. Inhibition by L-ascorbic acid and other antioxidants of the 2.2'-azino-bis(3-ethylbenzthiazoline-6-sulfonic acid) oxidation catalyzed by peroxidase: a new approach for determining total antioxidant status of foods. Anal Biochem. 1996 May 1;236(2):255-61. doi: 10.1006/abio.1996.0164. PMID: 8660502.

Bánhegyi G, Loewus FA. Ascorbic acid catabolism: breakdown pathways in animals and plants. Vitamin C, function and biochemistry in animals and plants (Asard H., May JM, Smirnoff, N. eds.). 2004 Aug 2:35.

Barupal DK, Zhang Y, Shen T, Fan S, Roberts BS, Fitzgerald P, Wancewicz B, Valdiviez L, Wohlgemuth G, Byram G, Choy YY, Haffner B, Showalter MR, Vaniya A, Bloszies CS, Folz JS, Kind T, Flenniken AM, McKerlie C, Nutter LMJ, Lloyd KC, Fiehn O. A Comprehensive Plasma Metabolomics Dataset for a Cohort of Mouse Knockouts within the International Mouse Phenotyping Consortium. Metabolites. 2019 May 22;9(5):101. doi: 10.3390/metabo9050101. PMID: 31121816; PMCID: PMC6571919.

Bayes-Genis A, Docherty KF, Petrie MC, Januzzi JL, Mueller C, Anderson L, Bozkurt B, Butler J, Chioncel O, Cleland JGF, Christodorescu R, Del Prato S, Gustafsson F, Lam CSP, Moura B, Pop-Busui R, Seferovic P, Volterrani M, Vaduganathan M, Metra M, Rosano G. Practical algorithms for early diagnosis of heart failure and heart stress using NT-proBNP: A clinical consensus statement from the Heart Failure Association of the ESC. Eur J Heart Fail. 2023 Sep 15. doi: 10.1002/ejhf.3036. Epub ahead of print. PMID: 37712339.

Benzie IF, Strain JJ. The ferric reducing ability of plasma (FRAP) as a measure of "antioxidant power": the FRAP assay. Anal Biochem. 1996 Jul 15;239(1):70-6. doi: 10.1006/abio.1996.0292. PMID: 8660627.

Birkeland KI, Bodegard J, Norhammar A, Kuiper JG, Georgiado E, Beekman-Hendriks WL, Thuresson M, Pignot M, Herings RMC, Kooy A. How representative of a general type 2 diabetes population are patients included in cardiovascular outcome trials with SGLT-2 inhibitors? A large European observational study. Diabetes Obes Metab. 2019 Apr;21(4):968-974. doi: 10.1111/dom.13612. Epub 2019 Jan 4. PMID: 30537226; PMCID: PMC6590461.

Boden G, Homko C, Barrero CA, Stein TP, Chen X, Cheung P, Fecchio C, Koller S, Merali S. Excessive caloric intake acutely causes oxidative stress, GLUT4 carbonylation, and insulin resistance in healthy men. Sci Transl Med. 2015 Sep 9;7(304):304re7. doi: 10.1126/scitranslmed.aac4765. PMID: 26355033; PMCID: PMC5600191.

Bolsoni-Lopes A, Festuccia WT, Chimin P, Farias TS, Torres-Leal FL, Cruz MM, Andrade PB, Hirabara SM, Lima FB, Alonso-Vale MI. Palmitoleic acid (n-7) increases white adipocytes GLUT4 content and glucose uptake in association with AMPK activation. Lipids Health Dis. 2014 Dec 20;13:199. doi: 10.1186/1476-511X-13-199. PMID: 25528561; PMCID: PMC4364637.

Burger M, Schaller DJ. Metabolic Acidosis. 2023 Jul 17. In: StatPearls [Internet]. Treasure Island (FL): StatPearls Publishing; 2023 Jan. PMID: 29489167.

Butler J, Anker SD, Filippatos G, Khan MS, Ferreira JP, Pocock SJ, Giannetti N, Januzzi JL, Piña IL, Lam CSP, Ponikowski P, Sattar N, Verma S, Brueckmann M, Jamal W,

Vedin O, Peil B, Zeller C, Zannad F, Packer M; EMPEROR-Reduced Trial Committees and Investigators. Empagliflozin and health-related quality of life outcomes in patients with heart failure with reduced ejection fraction: the EMPEROR-Reduced trial. Eur Heart J. 2021 Mar 31;42(13):1203-1212. doi: 10.1093/eurheartj/ehaa1007. PMID: 33420498; PMCID: PMC8014525.

Campos C, Guzmán R, López-Fernández E, Casado A. Evaluation of the copper(II) reduction assay using bathocuproinedisulfonic acid disodium salt for the total antioxidant capacity assessment: the CUPRAC-BCS assay. Anal Biochem. 2009 Sep 1;392(1):37-44. doi: 10.1016/j.ab.2009.05.024. Epub 2009 May 21. PMID: 19464250.

Centers for Disease Control and Prevention. National Diabetes Statistics Report website. https://www.cdc.gov/diabetes/data/statistics-report/index.html. Accessed 09/12/2023.

Chiofalo B, Fazio E, Lombardi P, Cucinotta S, Mastellone V, Di Rosa AR, Cravana C. Effects of dietary protein and fat concentrations on hormonal and oxidative blood stress biomarkers in guide dogs during training. J Vet Behav. 2020 June;37:86-92. doi: 10.1016/j.jveb.2019.12.003.

Clark A, Jones LC, de Koning E, Hansen BC, Matthews DR. Decreased insulin secretion in type 2 diabetes: a problem of cellular mass or function? Diabetes. 2001 Feb;50 Suppl 1:S169-71. doi: 10.2337/diabetes.50.2007.s169. PMID: 11272183.

Cowie MR, Fisher M. SGLT-2 inhibitors: mechanisms of cardiovascular benefit beyond glycaemic control. Nat Rev Cardiol. 2020 Dec;17(12):761-772. doi: 10.1038/s41569-020-0406-8. Epub 2020 Jul 14. PMID: 32665641.

Cruz MM, Lopes AB, Crisma AR, de Sá RCC, Kuwabara WMT, Curi R, de Andrade PBM, Alonso-Vale MIC. Palmitoleic acid (16:1n7) increases oxygen consumption, fatty acid oxidation and ATP content in white adipocytes. Lipids Health Dis. 2018 Mar 20;17(1):55. doi: 10.1186/s12944-018-0710-z. PMID: 29554895; PMCID: PMC5859716.

Da Costa CM, Dos Santos RCC, Lima ES. A simple automated procedure for thiol measurement in human serum samples. J. Bras. Patol. Med. Lab. 2006;42:345–350. doi: 10.1590/S1676-24442006000500006.

Diabetes Prevention Program Research Group. Long-term effects of lifestyle intervention or metformin on diabetes development and microvascular complications over 15-year follow-up: the Diabetes Prevention Program Outcomes Study. Lancet Diabetes Endocrinol. 2015 Nov;3(11):866-75. doi: 10.1016/S2213-8587(15)00291-0. Epub 2015 Sep 13. PMID: 26377054; PMCID: PMC4623946.

Domenig O, Manzel A, Grobe N, Königshausen E, Kaltenecker CC, Kovarik JJ, Stegbauer J, Gurley SB, van Oyen D, Antlanger M, Bader M, Motta-Santos D, Santos RA, Elased KM, Säemann MD, Linker RA, Poglitsch M. Neprilysin is a Mediator of Alternative Renin-Angiotensin-System Activation in the Murine and Human Kidney. Sci

Rep. 2016 Sep 21;6:33678. doi: 10.1038/srep33678. PMID: 27649628; PMCID: PMC5030486.

EMPA-KIDNEY Collaborative Group. Design, recruitment, and baseline characteristics of the EMPA-KIDNEY trial. Nephrol Dial Transplant. 2022 Jun 23;37(7):1317-1329. doi: 10.1093/ndt/gfac040. PMID: 35238940; PMCID: PMC9217655.

Erel O. A new automated colorimetric method for measuring total oxidant status. Clin Biochem. 2005 Dec;38(12):1103-11. doi: 10.1016/j.clinbiochem.2005.08.008. Epub 2005 Oct 7. PMID: 16214125.

Fiehn O, Wohlgemuth G, Scholz M, Kind T, Lee DY, Lu Y, Moon S, Nikolau B. Quality control for plant metabolomics: reporting MSI-compliant studies. Plant J. 2008 Feb;53(4):691-704. doi: 10.1111/j.1365-313X.2007.03387.x. PMID: 18269577.

Fiehn O. Metabolomics by Gas Chromatography-Mass Spectrometry: Combined Targeted and Untargeted Profiling. Curr Protoc Mol Biol. 2016 Apr 1;114:30.4.1-30.4.32. doi: 10.1002/0471142727.mb3004s114. PMID: 27038389; PMCID: PMC4829120.

Florensa-Zanuy E, Garro-Martínez E, Adell A, Castro E, Díaz Á, Pazos Á, Mac-Dowell KS, Martín-Hernández D, Pilar-Cuéllar F. Cannabidiol antidepressant-like effect in the lipopolysaccharide model in mice: Modulation of inflammatory pathways. Biochem Pharmacol. 2021 Mar;185:114433. doi: 10.1016/j.bcp.2021.114433. Epub 2021 Jan 26. PMID: 33513342.

Frühbeck G, Méndez-Giménez L, Fernández-Formoso JA, Fernández S, Rodríguez A. Regulation of adipocyte lipolysis. Nutr Res Rev. 2014 Jun;27(1):63-93. doi: 10.1017/S095442241400002X. Epub 2014 May 28. PMID: 24872083.

Giebelhaus RT, Sorochan Armstrong MD, de la Mata AP, Harynuk JJ. Untargeted region of interest selection for gas chromatography - mass spectrometry data using a pseudo F-ratio moving window. J Chromatogr A. 2022 Oct 25;1682:463499. doi: 10.1016/j.chroma.2022.463499. Epub 2022 Sep 13. PMID: 36126562.

Giebelhaus RT, Erland LAE, Murch SJ. HormonomicsDB: a novel workflow for the untargeted analysis of plant growth regulators and hormones. 2022. F1000 11.

González-Arostegui LG, Muñoz-Prieto A, Tvarijonaviciute A, Cerón JJ, Rubio CP. Measurement of Redox Biomarkers in the Whole Blood and Red Blood Cell Lysates of Dogs. Antioxidants (Basel). 2022 Feb 19;11(2):424. doi: 10.3390/antiox11020424. PMID: 35204305; PMCID: PMC8869394.

Grundy SM, Cleeman JI, Daniels SR, Donato KA, Eckel RH, Franklin BA, Gordon DJ, Krauss RM, Savage PJ, Smith SC Jr, Spertus JA, Costa F; American Heart Association; National Heart, Lung, and Blood Institute. Diagnosis and management of the metabolic syndrome: an American Heart Association/National Heart, Lung, and Blood Institute Scientific Statement. Circulation. 2005 Oct 25;112(17):2735-52. doi:

10.1161/CIRCULATIONAHA.105.169404. Epub 2005 Sep 12. Erratum in: Circulation. 2005 Oct 25;112(17):e298. PMID: 16157765.

Guo Z, Poglitsch M, McWhinney BC, Ungerer JPJ, Ahmed AH, Gordon RD, Wolley M, Stowasser M. Measurement of Equilibrium Angiotensin II in the Diagnosis of Primary Aldosteronism. Clin Chem. 2020 Mar 1;66(3):483-492. doi: 10.1093/clinchem/hvaa001. PMID: 32068832.

Heerspink HJL, Stefánsson BV, Correa-Rotter R, Chertow GM, Greene T, Hou FF, Mann JFE, McMurray JJV, Lindberg M, Rossing P, Sjöström CD, Toto RD, Langkilde AM, Wheeler DC; DAPA-CKD Trial Committees and Investigators. Dapagliflozin in Patients with Chronic Kidney Disease. N Engl J Med. 2020 Oct 8;383(15):1436-1446. doi: 10.1056/NEJMoa2024816. Epub 2020 Sep 24. PMID: 32970396.

Hishikawa D, Hashidate T, Shimizu T, Shindou H. Diversity and function of membrane glycerophospholipids generated by the remodeling pathway in mammalian cells. J Lipid Res. 2014 May;55(5):799-807. doi: 10.1194/jlr.R046094. Epub 2014 Mar 19. Erratum in: J Lipid Res. 2014 Nov;55(11):2444. PMID: 24646950; PMCID: PMC3995458.

Hooper L, Martin N, Jimoh OF, Kirk C, Foster E, Abdelhamid AS. Reduction in saturated fat intake for cardiovascular disease. Cochrane Database Syst Rev. 2020 May 19;5(5):CD011737. doi: 10.1002/14651858.CD011737.pub2. Update in: Cochrane Database Syst Rev. 2020 Aug 21;8:CD011737. PMID: 32428300; PMCID: PMC7388853.

Hussain A, Sun W, Deswal A, de Lemos JA, McEvoy JW, Hoogeveen RC, Matsushita K, Aguilar D, Bozkurt B, Virani SS, Shah AM, Selvin E, Ndumule C, Ballantyne CM, Nambi V. Association of NT-ProBNP, Blood Pressure, and Cardiovascular Events: The ARIC Study. J Am Coll Cardiol. 2021 Feb 9;77(5):559-571. doi: 10.1016/j.jacc.2020.11.063. PMID: 33538254; PMCID: PMC7945981.

Iennarella-Servantez CA, Kathrani A, Sahoo DK, Long EK, Zdyrski C, Gabriel V, Bedos L, Mao S, Bourgois-Mochel A, Resop MJ, Rund LR, Rossoni Serao M, Jergens AE, Mochel JP and Allenspach K. Diet-Induced Clinical Responsiveness of Translational Dog Model for Human Western Diet (WD)-Related Disease Research. J Anim Sci. 2021 Nov;99(3):58-59. doi: 10.1093/jas/skab235.104.

Inzucchi SE, Fitchett D, Jurišić-Eržen D, Woo V, Hantel S, Janista C, Kaspers S, George JT, Zinman B; EMPA-REG OUTCOME® Investigators. Are the cardiovascular and kidney benefits of empagliflozin influenced by baseline glucose-lowering therapy? Diabetes Obes Metab. 2020 Apr;22(4):631-639. doi: 10.1111/dom.13938. Epub 2020 Jan 3. PMID: 31789445.

Jang IS, Yoon WK, Choi EW. N-terminal pro-B-type natriuretic peptide levels in normotensive and hypertensive dogs with myxomatous mitral valve disease stage B. Ir

Vet J. 2023 Feb 8;76(1):3. doi: 10.1186/s13620-023-00233-0. PMID: 36755290; PMCID: PMC9906826.

Jocelyn PC. Spectrophotometric assay of thiols. Methods Enzymol. 1987;143:44-67. doi: 10.1016/0076-6879(87)43013-9. PMID: 3657559.

Kadowaki T, Maegawa H, Watada H, Yabe D, Node K, Murohara T, Wada J. Interconnection between cardiovascular, renal and metabolic disorders: A narrative review with a focus on Japan. Diabetes Obes Metab. 2022 Dec;24(12):2283-2296. doi: 10.1111/dom.14829. Epub 2022 Aug 25. PMID: 35929483; PMCID: PMC9804928.

Kalaitzidis R, Tsimihodimos V, Bairaktari E, Siamopoulos KC, Elisaf M. Disturbances of phosphate metabolism: another feature of metabolic syndrome. Am J Kidney Dis. 2005 May;45(5):851-8. doi: 10.1053/j.ajkd.2005.01.005. PMID: 15861350.

Kapun AP, Salobir J, Levart A, Kotnik T, Svete AN. Oxidative stress markers in canine atopic dermatitis. Res Vet Sci. 2012 Jun;92(3):469-70. doi: 10.1016/j.rvsc.2011.04.014. Epub 2011 May 23. PMID: 21601227.

Khan MS, Fonarow GC, McGuire DK, Hernandez AF, Vaduganathan M, Rosenstock J, Handelsman Y, Verma S, Anker SD, McMurray JJV, Kosiborod MN, Butler J. Glucagon-Like Peptide 1 Receptor Agonists and Heart Failure: The Need for Further Evidence Generation and Practice Guidelines Optimization. Circulation. 2020 Sep 22;142(12):1205-1218. doi: 10.1161/CIRCULATIONAHA.120.045888. Epub 2020 Sep 21. PMID: 32955939.

Kimura T, Hashimoto Y, Tanaka M, Asano M, Yamazaki M, Oda Y, Toda H, Marunaka Y, Nakamura N, Fukui M. Sodium-chloride Difference and Metabolic Syndrome: A Population-based Large-scale Cohort Study. Intern Med. 2016;55(21):3085-3090. doi: 10.2169/internalmedicine.55.7000. Epub 2016 Nov 1. PMID: 27803399; PMCID: PMC5140854.

Kind T, Wohlgemuth G, Lee DY, Lu Y, Palazoglu M, Shahbaz S, Fiehn O. FiehnLib: mass spectral and retention index libraries for metabolomics based on quadrupole and time-of-flight gas chromatography/mass spectrometry. Anal Chem. 2009 Dec 15;81(24):10038-48. doi: 10.1021/ac9019522. PMID: 19928838; PMCID: PMC2805091.

Kind T, Liu KH, Lee DY, DeFelice B, Meissen JK, Fiehn O. LipidBlast in silico tandem mass spectrometry database for lipid identification. Nat Methods. 2013 Aug;10(8):755-8. doi: 10.1038/nmeth.2551. Epub 2013 Jun 30. PMID: 23817071; PMCID: PMC3731409.

Kosiborod MN, Abildstrøm SZ, Borlaug BA, Butler J, Rasmussen S, Davies M, Hovingh GK, Kitzman DW, Lindegaard ML, Møller DV, Shah SJ, Treppendahl MB, Verma S, Abhayaratna W, Ahmed FZ, Chopra V, Ezekowitz J, Fu M, Ito H, Lelonek M, Melenovsky V, Merkely B, Núñez J, Perna E, Schou M, Senni M, Sharma K, Van der Meer P, von Lewinski D, Wolf D, Petrie MC; STEP-HFpEF Trial Committees and Investigators.

Semaglutide in Patients with Heart Failure with Preserved Ejection Fraction and Obesity. N Engl J Med. 2023 Sep 21;389(12):1069-1084. doi: 10.1056/NEJMoa2306963. Epub 2023 Aug 25. PMID: 37622681.

Lahm Cardoso JM, Fagnani R, Zaghi Cavalcante C, de Souza Zanutto M, Júnior AZ, Holsback da Silveira Fertonani L, Calesso JR, Melussi M, Pinheiro Costa H, Yudi Hashizume E. Blood Pressure, Serum Glucose, Cholesterol, and Triglycerides in Dogs with Different Body Scores. Vet Med Int. 2016;2016:8675283. doi: 10.1155/2016/8675283. Epub 2016 Dec 12. PMID: 28058131; PMCID: PMC5183795.

Lambert DC, Kane J, Slaton A, Abramowitz MK. Associations of Metabolic Syndrome and Abdominal Obesity with Anion Gap Metabolic Acidosis among US Adults. Kidney360. 2022 Jul 13;3(11):1842-1851. doi: 10.34067/KID.0002402022. PMID: 36514392; PMCID: PMC9717647.

Larner CD. High performance lipoprotein profiling for cardiovascular risk assessment. PhD thesis, Texas A&M University, 2012.

Littman MP. Spontaneous systemic hypertension in 24 cats. J Vet Intern Med. 1994 Mar-Apr;8(2):79-86. doi: 10.1111/j.1939-1676.1994.tb03202.x. PMID: 8046680.

Lyu Y, Liu D, Nguyen P, Peters I, Heilmann RM, Fievez V, Hemeryck LY, Hesta M. Differences in Metabolic Profiles of Healthy Dogs Fed a High-Fat vs. a High-Starch Diet. Front Vet Sci. 2022 Feb 17;9:801863. doi: 10.3389/fvets.2022.801863. PMID: 35252418; PMCID: PMC8891928.

Matsuzawa-Nagata N, Takamura T, Ando H, Nakamura S, Kurita S, Misu H, Ota T, Yokoyama M, Honda M, Miyamoto K, Kaneko S. Increased oxidative stress precedes the onset of high-fat diet-induced insulin resistance and obesity. Metabolism. 2008 Aug;57(8):1071-7. doi: 10.1016/j.metabol.2008.03.010. PMID: 18640384.

Matyash V, Liebisch G, Kurzchalia TV, Shevchenko A, Schwudke D. Lipid extraction by methyl-tert-butyl ether for high-throughput lipidomics. J Lipid Res. 2008 May;49(5):1137-46. doi: 10.1194/jlr.D700041-JLR200. Epub 2008 Feb 16. PMID: 18281723; PMCID: PMC2311442.

McMurray JJV, DeMets DL, Inzucchi SE, Køber L, Kosiborod MN, Langkilde AM, Martinez FA, Bengtsson O, Ponikowski P, Sabatine MS, Sjöstrand M, Solomon SD; DAPA-HF Committees and Investigators. The Dapagliflozin And Prevention of Adverse-outcomes in Heart Failure (DAPA-HF) trial: baseline characteristics. Eur J Heart Fail. 2019 Nov;21(11):1402-1411. doi: 10.1002/ejhf.1548. Epub 2019 Jul 15. PMID: 31309699.

Minamoto T, Walzem RL, Hamilton AJ, Hill SL, Payne HR, Lidbury JA, Suchodolski JS, Steiner JM. Altered lipoprotein profiles in cats with hepatic lipidosis. J Feline Med Surg. 2019 Apr;21(4):363-372. doi: 10.1177/1098612X18780060. Epub 2018 Jun 4. PMID: 29860906.

Mochel JP, Teng CH, Peyrou M, Giraudel J, Danhof M, Rigel DF. Sacubitril/valsartan (LCZ696) significantly reduces aldosterone and increases cGMP circulating levels in a canine model of RAAS activation. Eur J Pharm Sci. 2019 Feb 1;128:103-111. doi: 10.1016/j.ejps.2018.11.037. Epub 2018 Nov 30. PMID: 30508581.

Mochel JP, Danhof M. Chronobiology and Pharmacologic Modulation of the Renin-Angiotensin-Aldosterone System in Dogs: What Have We Learned? Rev Physiol Biochem Pharmacol. 2015;169:43-69. doi: 10.1007/112_2015_27. PMID: 26428686.

Mochel JP, Fink M, Peyrou M, Soubret A, Giraudel JM, Danhof M. Pharmacokinetic/Pharmacodynamic Modeling of Renin-Angiotensin Aldosterone Biomarkers Following Angiotensin-Converting Enzyme (ACE) Inhibition Therapy with Benazepril in Dogs. Pharm Res. 2015 Jun;32(6):1931-46. doi: 10.1007/s11095-014-1587-9. Epub 2014 Dec 2. PMID: 25446774.

Moinard A, Payen C, Ouguerram K, André A, Hernandez J, Drut A, Biourge VC, Suchodolski JS, Flanagan J, Nguyen P, Leray V. Effects of High-Fat Diet at Two Energetic Levels on Fecal Microbiota, Colonic Barrier, and Metabolic Parameters in Dogs. Front Vet Sci. 2020 Sep 25;7:566282. doi: 10.3389/fvets.2020.566282. PMID: 33102570; PMCID: PMC7545960.

Nagaoka D, Mitsuhashi Y, Angell R, Bigley KE, Bauer JE. Re-induction of obese body weight occurs more rapidly and at lower caloric intake in beagles. J Anim Physiol Anim Nutr (Berl). 2010 Jun;94(3):287-92. doi: 10.1111/j.1439-0396.2008.00908.x. Epub 2009 Mar 31. PMID: 19364373.

National Health and Nutrition Examination Survey (NHANES 2015-2016: Males and Females over 20 years). https://www.ars.usda.gov/northeast-area/beltsville-md-bhnrc/beltsville-human-nutrition-research-center/food-surveys-research-group/docs/temp-wweia-usual-intake-data-tables/.

National Heart, Lung, and Blood Institute (NHLBI). What is Metabolic Syndrome? https://www.nhlbi.nih.gov/health/metabolic-syndrome#:~:text=Metabolic%20syndrome%20is%20a%20group,also%20called%20insulin%20resistance%20syndrome. Last updated May 18, 2022.

Ndumele CE, Rangaswami J, Chow SL, Neeland IJ, Tuttle KR, Khan SS, Coresh J, Mathew RO, Baker-Smith CM, Carnethon MR, Despres JP, Ho JE, Joseph JJ, Kernan WN, Khera A, Kosiborod MN, Lekavich CL, Lewis EF, Lo KB, Ozkan B, Palaniappan LP, Patel SS, Pencina MJ, Powell-Wiley TM, Sperling LS, Virani SS, Wright JT, Rajgopal Singh R, Elkind MSV; American Heart Association. Cardiovascular-Kidney-Metabolic Health: A Presidential Advisory From the American Heart Association. Circulation. 2023 Oct 9. doi: 10.1161/CIR.0000000000001184. Epub ahead of print. PMID: 37807924.

Neal B, Perkovic V, Mahaffey KW, de Zeeuw D, Fulcher G, Erondu N, Shaw W, Law G, Desai M, Matthews DR; CANVAS Program Collaborative Group. Canagliflozin and

Cardiovascular and Renal Events in Type 2 Diabetes. N Engl J Med. 2017 Aug 17;377(7):644-657. doi: 10.1056/NEJMoa1611925. Epub 2017 Jun 12. PMID: 28605608.

Newsome PN, Ambery P. Incretins (GLP-1 receptor agonists and dual/triple agonists) and the liver. J Hepatol. 2023 Aug 9:S0168-8278(23)05046-8. doi: 10.1016/j.jhep.2023.07.033. Epub ahead of print. PMID: 37562748.

Oyama K, Raz I, Cahn A, Kuder J, Murphy SA, Bhatt DL, Leiter LA, McGuire DK, Wilding JPH, Park KS, Goudev A, Diaz R, Špinar J, Gause-Nilsson IAM, Mosenzon O, Sabatine MS, Wiviott SD. Obesity and effects of dapagliflozin on cardiovascular and renal outcomes in patients with type 2 diabetes mellitus in the DECLARE-TIMI 58 trial. Eur Heart J. 2022 Aug 14;43(31):2958-2967. doi: 10.1093/eurheartj/ehab530. PMID: 34427295.

Packer M. SGLT-2 Inhibitors Produce Cardiorenal Benefits by Promoting Adaptive Cellular Reprogramming to Induce a State of Fasting Mimicry: A Paradigm Shift in Understanding Their Mechanism of Action. Diabetes Care. 2020 Mar;43(3):508-511. doi: 10.2337/dci19-0074. PMID: 32079684.

Packer M, Butler J, Filippatos G, Zannad F, Ferreira JP, Zeller C, Brueckmann M, Jamal W, Pocock SJ, Anker SD; EMPEROR Trial Committees and Investigators. Design of a prospective patient-level pooled analysis of two parallel trials of empagliflozin in patients with established heart failure. Eur J Heart Fail. 2020 Dec;22(12):2393-2398. doi: 10.1002/ejhf.2065. Epub 2020 Dec 14. PMID: 33251659; PMCID: PMC7898542.

Peña C, Suarez L, Bautista-Castaño I, Juste MC, Carretón E, Montoya-Alonso JA. Effects of low-fat high-fiber diet and mitratapide on body weight reduction, blood pressure and metabolic parameters in obese dogs. J Vet Med Sci. 2014 Sep;76(9):1305-8. doi: 10.1292/jvms.13-0475. Epub 2014 Jun 11. PMID: 24920548; PMCID: PMC4197164.

Perkovic V, Jardine MJ, Neal B, Bompoint S, Heerspink HJL, Charytan DM, Edwards R, Agarwal R, Bakris G, Bull S, Cannon CP, Capuano G, Chu PL, de Zeeuw D, Greene T, Levin A, Pollock C, Wheeler DC, Yavin Y, Zhang H, Zinman B, Meininger G, Brenner BM, Mahaffey KW; CREDENCE Trial Investigators. Canagliflozin and Renal Outcomes in Type 2 Diabetes and Nephropathy. N Engl J Med. 2019 Jun 13;380(24):2295-2306. doi: 10.1056/NEJMoa1811744. Epub 2019 Apr 14. PMID: 30990260.

Persson F, Nyström T, Jørgensen ME, Carstensen B, Gulseth HL, Thuresson M, Fenici P, Nathanson D, Eriksson JW, Norhammar A, Bodegard J, Birkeland KI. Dapagliflozin is associated with lower risk of cardiovascular events and all-cause mortality in people with type 2 diabetes (CVD-REAL Nordic) when compared with dipeptidyl peptidase-4 inhibitor therapy: A multinational observational study. Diabetes Obes Metab. 2018

Feb;20(2):344-351. doi: 10.1111/dom.13077. Epub 2017 Sep 8. PMID: 28771923; PMCID: PMC5811811.

Rix I, Nexøe-Larsen C, Bergmann NC, Lund A, Knop FK. Glucagon Physiology. 2019 Jul 16. In: Feingold KR, Anawalt B, Blackman MR, Boyce A, Chrousos G, Corpas E, de Herder WW, Dhatariya K, Dungan K, Hofland J, Kalra S, Kaltsas G, Kapoor N, Koch C, Kopp P, Korbonits M, Kovacs CS, Kuohung W, Laferrère B, Levy M, McGee EA, McLachlan R, New M, Purnell J, Sahay R, Shah AS, Singer F, Sperling MA, Stratakis CA, Trence DL, Wilson DP, editors. Endotext [Internet]. South Dartmouth (MA): MDText.com, Inc.; 2000–. PMID: 25905350.

Rubio CP, Hernández-Ruiz J, Martinez-Subiela S, Tvarijonaviciute A, Arnao MB, Ceron JJ. Validation of three automated assays for total antioxidant capacity determination in canine serum samples. J Vet Diagn Invest. 2016 Nov;28(6):693-698. doi: 10.1177/1040638716664939. Epub 2016 Oct 3. PMID: 27698166.

Rubio CP, Martinez-Subiela S, Hernández-Ruiz J, Tvarijonaviciute A, Ceron JJ. Analytical validation of an automated assay for ferric-reducing ability of plasma in dog serum. J Vet Diagn Invest. 2017 Jul;29(4):574-578. doi: 10.1177/1040638717693883. Epub 2017 Apr 19. PMID: 28424022.

Rubio CP, Tvarijonaviciute A, Caldin M, Hernández-Ruiz J, Cerón JJ, Martínez-Subiela S, Tecles F. Stability of biomarkers of oxidative stress in canine serum. Res Vet Sci. 2018 Dec;121:85-93. doi: 10.1016/j.rvsc.2018.09.007. Epub 2018 Sep 28. PMID: 30359815.

Schneider BK, Ward J, Sotillo S, Garelli-Paar C, Guillot E, Prikazsky M, Mochel JP. Breakthrough: a first-in-class virtual simulator for dose optimization of ACE inhibitors in translational cardiovascular medicine. Sci Rep. 2023 Feb 26;13(1):3300. doi: 10.1038/s41598-023-30453-x. PMID: 36843132; PMCID: PMC9968717.

Schneider B, Balbas-Martinez V, Jergens AE, Troconiz IF, Allenspach K, Mochel JP. Model-Based Reverse Translation Between Veterinary and Human Medicine: The One Health Initiative. CPT Pharmacometrics Syst Pharmacol. 2018 Feb;7(2):65-68. doi: 10.1002/psp4.12262. Epub 2017 Nov 27. PMID: 29178333; PMCID: PMC5824107.

Sharma S, Hashmi MF, Aggarwal S. Hyperchloremic Acidosis. 2023 May 8. In: StatPearls [Internet]. Treasure Island (FL): StatPearls Publishing; 2023 Jan–PMID: 29493965.

Singletary GE, Morris NA, Lynne O'Sullivan M, Gordon SG, Oyama MA. Prospective evaluation of NT-proBNP assay to detect occult dilated cardiomyopathy and predict survival in Doberman Pinschers. J Vet Intern Med. 2012 Nov-Dec;26(6):1330-6. doi: 10.1111/j.1939-1676.2012.1000.x. Epub 2012 Sep 24. PMID: 22998090.

Sinkov NA, Harynuk JJ. Cluster resolution: a metric for automated, objective and optimized feature selection in chemometric modeling. Talanta. 2011 Jan 30;83(4):1079-87. doi: 10.1016/j.talanta.2010.10.025. Epub 2010 Oct 27. PMID: 21215842.

Siri-Tarino PW, Sun Q, Hu FB, Krauss RM. Saturated fat, carbohydrate, and cardiovascular disease. Am J Clin Nutr. 2010 Mar;91(3):502-9. doi: 10.3945/ajcn.2008.26285. Epub 2010 Jan 20. PMID: 20089734; PMCID: PMC2824150.

Skogerson K, Wohlgemuth G, Barupal DK, Fiehn O. The volatile compound BinBase mass spectral database. BMC Bioinformatics. 2011 Aug 4;12:321. doi: 10.1186/1471-2105-12-321. PMID: 21816034; PMCID: PMC3199763.

Sostare J, Di Guida R, Kirwan J, Chalal K, Palmer E, Dunn WB, Viant MR. Comparison of modified Matyash method to conventional solvent systems for polar metabolite and lipid extractions. Anal Chim Acta. 2018 Dec 11;1037:301-315. doi: 10.1016/j.aca.2018.03.019. Epub 2018 Apr 5. Erratum in: Anal Chim Acta. 2019 Dec 24;1091:169. PMID: 30292307.

Sotillo S, Ward JL, Guillot E, Domenig O, Yuan L, Smith JS, Gabriel V, Iennarella-Servantez CA, Mochel JP. Dose-response of benazepril on biomarkers of the classical and alternative pathways of the renin-angiotensin-aldosterone system in dogs. Sci Rep. 2023 Feb 15;13(1):2684. doi: 10.1038/s41598-023-29771-x. PMID: 36792677; PMCID: PMC9932142.

Stoian M, Stoica V. The role of distubances of phosphate metabolism in metabolic syndrome. Maedica (Bucur). 2014 Sep;9(3):255-60. PMID: 25705287; PMCID: PMC4305993.

Sumner LW, Amberg A, Barrett D, Beale MH, Beger R, Daykin CA, Fan TW, Fiehn O, Goodacre R, Griffin JL, Hankemeier T, Hardy N, Harnly J, Higashi R, Kopka J, Lane AN, Lindon JC, Marriott P, Nicholls AW, Reily MD, Thaden JJ, Viant MR. Proposed minimum reporting standards for chemical analysis Chemical Analysis Working Group (CAWG) Metabolomics Standards Initiative (MSI). Metabolomics. 2007 Sep;3(3):211-221. doi: 10.1007/s11306-007-0082-2. PMID: 24039616; PMCID: PMC3772505.

Sun H, Zhang Q, Xu C, Mao A, Zhao H, Chen M, Sun W, Li G, Zhang T. Different Diet Energy Levels Alter Body Condition, Glucolipid Metabolism, Fecal Microbiota and Metabolites in Adult Beagle Dogs. Metabolites. 2023 Apr 13;13(4):554. doi: 10.3390/metabo13040554. PMID: 37110212; PMCID: PMC10143615.

Sun K, Su T, Li M, Xu B, Xu M, Lu J, Liu J, Bi Y, Ning G. Serum potassium level is associated with metabolic syndrome: a population-based study. Clin Nutr. 2014 Jun;33(3):521-7. doi: 10.1016/j.clnu.2013.07.010. Epub 2013 Jul 17. PMID: 23910935.

Surjana D, Halliday GM, Damian DL. Role of nicotinamide in DNA damage, mutagenesis, and DNA repair. J Nucleic Acids. 2010 Jul 25;2010:157591. doi: 10.4061/2010/157591. PMID: 20725615; PMCID: PMC2915624.

Tatzber F, Griebenow S, Wonisch W, Winkler R. Dual method for the determination of peroxidase activity and total peroxides-iodide leads to a significant increase of peroxidase activity in human sera. Anal Biochem. 2003 May 15;316(2):147-53. doi: 10.1016/s0003-2697(02)00652-8. PMID: 12711334.

Tropf M, Nelson OL, Lee PM, Weng HY. Cardiac and Metabolic Variables in Obese Dogs. J Vet Intern Med. 2017 Jul;31(4):1000-1007. doi: 10.1111/jvim.14775. Epub 2017 Jun 13. PMID: 28608635; PMCID: PMC5508341.

Tsugawa H, Cajka T, Kind T, Ma Y, Higgins B, Ikeda K, Kanazawa M, VanderGheynst J, Fiehn O, Arita M. MS-DIAL: data-independent MS/MS deconvolution for comprehensive metabolome analysis. Nat Methods. 2015 Jun;12(6):523-6. doi: 10.1038/nmeth.3393. Epub 2015 May 4. PMID: 25938372; PMCID: PMC4449330.

Tvarijonaviciute A, Tecles F, Caldin M, Tasca S, Cerón J. Validation of spectrophotometric assays for serum paraoxonase type-1 measurement in dogs. Am J Vet Res. 2012 Jan;73(1):34-41. doi: 10.2460/ajvr.73.1.34. PMID: 22204286.

Tvarijonaviciute A, Ceron JJ, Holden SL, Cuthbertson DJ, Biourge V, Morris PJ, German AJ. Obesity-related metabolic dysfunction in dogs: a comparison with human metabolic syndrome. BMC Vet Res. 2012 Aug 28;8:147. doi: 10.1186/1746-6148-8-147. PMID: 22929809; PMCID: PMC3514388.

Ulmer CZ, Jones CM, Yost RA, Garrett TJ, Bowden JA. Optimization of Folch, Bligh-Dyer, and Matyash sample-to-extraction solvent ratios for human plasma-based lipidomics studies. Anal Chim Acta. 2018 Dec 11;1037:351-357. doi: 10.1016/j.aca.2018.08.004. Epub 2018 Aug 8. PMID: 30292311; PMCID: PMC6261534.

Vecchiato CG, Golinelli S, Pinna C, Pilla R, Suchodolski JS, Tvarijonaviciute A, Rubio CP, Dorato E, Delsante C, Stefanelli C, Pagani E, Fracassi F, Biagi G. Fecal microbiota and inflammatory and antioxidant status of obese and lean dogs, and the effect of caloric restriction. Front Microbiol. 2023 Jan 12;13:1050474. doi: 10.3389/fmicb.2022.1050474. PMID: 36713218; PMCID: PMC9878458.

Verk B, Nemec Svete A, Salobir J, Rezar V, Domanjko Petrič A. Markers of oxidative stress in dogs with heart failure. J Vet Diagn Invest. 2017 Sep;29(5):636-644. doi: 10.1177/1040638717711995. Epub 2017 Jun 4. PMID: 28580831.

Ward JL, Chou YY, Yuan L, Dorman KS, Mochel JP. Retrospective evaluation of a dose-dependent effect of angiotensin-converting enzyme inhibitors on long-term outcome in dogs with cardiac disease. J Vet Intern Med. 2021 Sep;35(5):2102-2111. doi: 10.1111/jvim.16236. Epub 2021 Aug 13. PMID: 34387901; PMCID: PMC8478030.

Ward JL, Guillot E, Domenig O, Ware WA, Yuan L, Mochel JP. Circulating renin-angiotensin-aldosterone system activity in cats with systemic hypertension or cardiomyopathy. J Vet Intern Med. 2022 May;36(3):897-909. doi: 10.1111/jvim.16401. Epub 2022 Mar 14. PMID: 35285549; PMCID: PMC9151484.

Wheeler DC, Stefansson BV, Batiushin M, Bilchenko O, Cherney DZI, Chertow GM, Douthat W, Dwyer JP, Escudero E, Pecoits-Filho R, Furuland H, Górriz JL, Greene T, Haller H, Hou FF, Kang SW, Isidto R, Khullar D, Mark PB, McMurray JJV, Kashihara N, Nowicki M, Persson F, Correa-Rotter R, Rossing P, Toto RD, Umanath K, Van Bui P, Wittmann I, Lindberg M, Sjöström CD, Langkilde AM, Heerspink HJL. The dapagliflozin and prevention of adverse outcomes in chronic kidney disease (DAPA-CKD) trial: baseline characteristics. Nephrol Dial Transplant. 2020 Oct 1;35(10):1700-1711. doi: 10.1093/ndt/gfaa234. PMID: 32862232; PMCID: PMC7538235.

Wilshaw J, Rosenthal SL, Wess G, Dickson D, Bevilacqua L, Dutton E, Deinert M, Abrantes R, Schneider I, Oyama MA, Gordon SG, Elliott J, Xia D, Boswood A. Accuracy of history, physical examination, cardiac biomarkers, and biochemical variables in identifying dogs with stage B2 degenerative mitral valve disease. J Vet Intern Med. 2021 Mar;35(2):755-770. doi: 10.1111/jvim.16083. Epub 2021 Mar 1. PMID: 33645846; PMCID: PMC7995403.

Witko-Sarsat V, Friedlander M, Capeillère-Blandin C, Nguyen-Khoa T, Nguyen AT, Zingraff J, Jungers P, Descamps-Latscha B. Advanced oxidation protein products as a novel marker of oxidative stress in uremia. Kidney Int. 1996 May;49(5):1304-13. doi: 10.1038/ki.1996.186. PMID: 8731095.

Xue J, Lu Y, Zou T, Shi W, Wang S, Cheng X, Wan J, Chen Y, Wang M, Wang Q, Yang X, Ding M, Qi Z, Ding Y, Hu M, Zhang X, Li H, Hu Y. A protein- and fiber-rich diet with astaxanthin alleviates high-fat diet-induced obesity in beagles. Front Nutr. 2022 Oct 24;9:1019615. doi: 10.3389/fnut.2022.1019615. PMID: 36352906; PMCID: PMC9637869.

Yoshino J, Mills KF, Yoon MJ, Imai S. Nicotinamide mononucleotide, a key NAD(+) intermediate, treats the pathophysiology of diet- and age-induced diabetes in mice. Cell Metab. 2011 Oct 5;14(4):528-36. doi: 10.1016/j.cmet.2011.08.014. PMID: 21982712; PMCID: PMC3204926.

Zinman B, Wanner C, Lachin JM, Fitchett D, Bluhmki E, Hantel S, Mattheus M, Devins T, Johansen OE, Woerle HJ, Broedl UC, Inzucchi SE; EMPA-REG OUTCOME Investigators. Empagliflozin, Cardiovascular Outcomes, and Mortality in Type 2 Diabetes. N Engl J Med. 2015 Nov 26;373(22):2117-28. doi: 10.1056/NEJMoa1504720. Epub 2015 Sep 17. PMID: 26378978.

Zoufaly A, Poglitsch M, Aberle JH, Hoepler W, Seitz T, Traugott M, Grieb A, Pawelka E, Laferl H, Wenisch C, Neuhold S, Haider D, Stiasny K, Bergthaler A, Puchhammer-Stoeckl E, Mirazimi A, Montserrat N, Zhang H, Slutsky AS, Penninger JM. Human recombinant soluble ACE2 in severe COVID-19. Lancet Respir Med. 2020 Nov;8(11):1154-1158. doi: 10.1016/S2213-2600(20)30418-5. Epub 2020 Sep 24. Erratum in: Lancet Respir Med. 2020 Nov;8(11):e78. PMID: 33131609; PMCID: PMC7515587.

TABLES

Table 1. Nutritional Characteristics (1A) and Composition (1B) of the Western Diet. Eighteen healthy adult Beagle dogs were fed a high-fat, high-monosaccharide, low-fiber Western diet (WD) adjusted from parameters of the National Health and Nutrition Examination Survey (NHANES) for a period of ten weeks. The dogs were provided with isocaloric feedings based on their individually calculated metabolizable energy. The diets were home cooked and offered to the dogs once daily in the morning, typically around 9 a.m.

1A.

PARAMETER	TARGET	ACTUAL
Energy (kcal)	1,000.0	1,000.3
Protein (g/Mcal)	40.1	40.3
Fat (g/Mcal)	40.8	40.9
CHO (g/Mcal)	118.3	117.9
Fiber (g/Mcal)	8.4	8.4
Sugar (g/Mcal)	51.4	51.4
Saturated fat (%)	37.0	36.4

1B.

INGREDIENT	g per 1,000 kcal
Ground beef, 80% lean	56.0
Egg protein powder	9.8
Bread brown	99.0
Bread white	70.0
Light corn syrup	47.0
Corn oil	11.0
Unsalted butter	15.5
Psyllium husk	3.0
Iodized salt	5.0
Balance.it® Canine K	14.4
Calcium/phosphate	2.3
Welactin Canine liquid	0.5
Fleet enema	1.0 (mL)

Table 2. Effect of the Western Diet Model on Biomarkers of the Renin-Angiotensin Aldosterone System (RAAS). Pharmacodynamic changes in both the classical and alternative arm of the RAAS after ten weeks of feeding with a high-fat, high-monosaccharide, low-fiber Western diet (WD), including: Angiotensin I (Ang I (1–10)), Angiotensin II (Ang II (1–8)), Angiotensin III (Ang III (2–8)), Angiotensin IV (Ang IV (3–8)), Angiotensin 1–7 (Ang1–7), and Angiotensin 1–5 (Ang1–5). Markers for renin (PRA–S) and angiotensin-converting enzyme (ACE–S) based on angiotensin were obtained from Ang II (1–8) and Ang I (1–10) levels by calculating their sum and ratio, respectively (Guo et al., 2020). Renin-independent alternative RAAS activation (ALT–S) was calculated using the formula [(Ang 1-7 + Ang 1-5) / (Ang I + Ang II + Ang 1-7 + Ang 1-5)], as previously described (Zoufaly et al., 2020).

VARIABLE	BAS1	BAS2	*P*-VALUE
Ang I (1–10)	100.7 (70.7-114.5)	71.6 (40.3-102.3)	0.30
Ang II (1–8)	68.8 (40.8-81.3)	45.4 (25.4-91.7)	0.62
Ang III (2–8)	14.8 (8.4-15.4)	11.0 (7.7-12.3)	0.68
Ang IV (3–8)	13.7 (10.3-15.8)	7.6 (5.5-11.6)	0.11
Ang (1–7)	25.5 (11.7-35.2)	17.1 (9.0-19.0)	0.42
Ang (1–5)	57.9 (34.7-70.6)	35.4 (25.1-54.2)	0.30
ACE–S	0.68 (0.57-0.72)	0.64 (0.52-0.68)	0.73
PRA–S	176.8 (121.8-194.5)	106.9 (67.5-196.5)	0.42
ALT–S	0.34 (0.28-0.38)	0.32 (0.27-0.39)	0.62

Table 3. Effect of the Western Diet Model on Circulating Lipoprotein Fractions. Lipoprotein profiles were produced by plotting the average intensity of fluorescence on the y-axis, while the actual centrifuge tube coordinates (mm) served as the x-axis. A unique numbering system was established for statistical examination. The area under the curve (AUC) of the total fluorescence trace and each segment were used to determine the total lipoprotein intensity and fractional intensities, respectively. Moreover, AUCs were calculated for high-density lipoproteins (HDLs) and low-density lipoproteins (LDLs), based on their density intervals. These AUC values were normalized using the total AUC and expressed as percentage, as previously presented by Minamoto et al. (2018).

VARIABLE	BAS1	BAS2	*P*-VALUE
HDL 2a (AUC%)	28.3 (26.4-28.8)	24.7 (21.8-27.1)	<0.001
HDL 2b (AUC%)	21.4 (18.4-23.3)	21.1 (19.2-22.2)	0.39
HDL 3a (AUC%)	25.1 (23.2-27.9)	24.6 (22.4-26.2)	0.14
HDL 3b (AUC%)	7.1 (6.0-8.0)	7.4 (6.5-8.7)	0.13
HDL 3c (AUC%)	1.2 (1.0-1.3)	1.3 (1.0-1.5)	0.61
HDL total (AUC%)	**84.2 (80.5-85.6)**	**81.1 (72.8-83.1)**	**<0.001**
LDL 1 (AUC%)	0.6 (0.5-0.8)	0.6 (0.5-0.7)	0.44
LDL 2 (AUC%)	1.4 (1.2-1.5)	1.5 (1.2-1.7)	0.30
LDL 3 (AUC%)	2.6 (2.4-3.5)	4.8 (3.9-6.9)	<0.001
LDL 4 (AUC%)	4.1 (3.7-4.9)	5.2 (4.4-6.8)	<0.001
LDL 5 (AUC%)	6.1 (4.9-6.7)	6.2 (5.0-7.4)	0.26
LDL total (AUC%)	**14.5 (13.0-17.0)**	**18.0 (15.5-24.5)**	**<0.001**

Figure 1. Rationale for the Use of SGLT-2i in CardioRenal Metabolic (CRM) Diseases. Molecular basis for the interrelationshipt between cardiovascular, renal and metabolic disoders. Adjusted and simplified from Kadowaki et al. (2022).

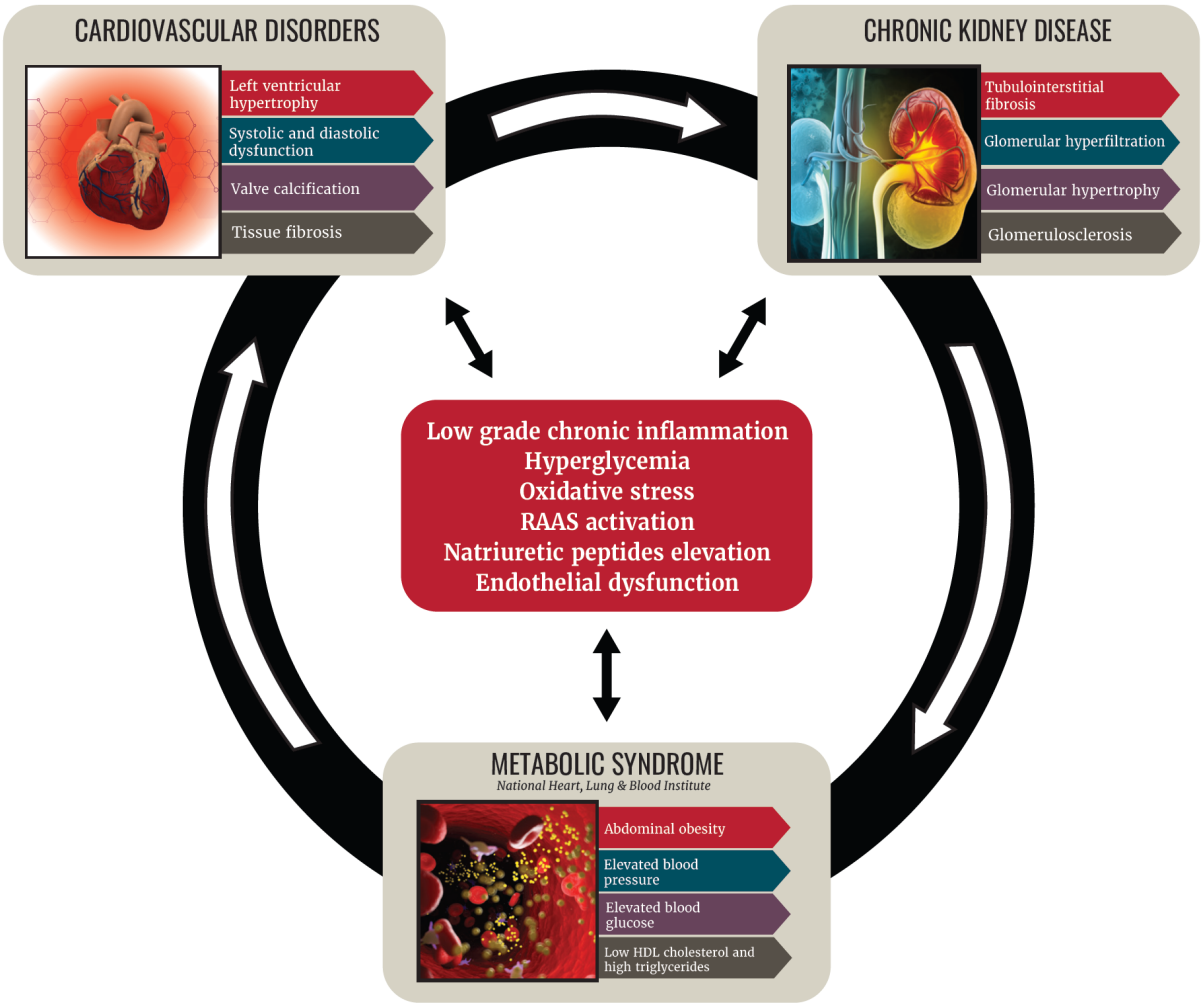

Figure 2. Experimental Study Design. Eighteen healthy adult Beagle dogs were fed a high-fat, high-monosaccharide, low-fiber western diet (WD) adjusted from parameters of the National Health and Nutrition Examination Survey (NHANES) for ten weeks. Blood samples were collected at baseline (***BAS1***) when dogs were fed their regular diet, and then again after ten weeks of WD feeding (***BAS2***) for measurement of complete blood count, standard chemistry panel, fasting blood glucose, glucagon and insulin, lipid profiling, renin-angiotensin aldosterone system biomarkers, NT-proBNP, oxidative stress biomarkers, and serum metabolomics. Voided urine and fecal samples were collected at ***BAS1*** and ***BAS2*** for the purpose of conducting urine metabolomics, including (1) General Metabolism; (2) Complex Lipids and (3) Biogenic Amines. Blood pressure was measured by a certified cardiologist utilizing a Doppler device. ACC: acclimatation.

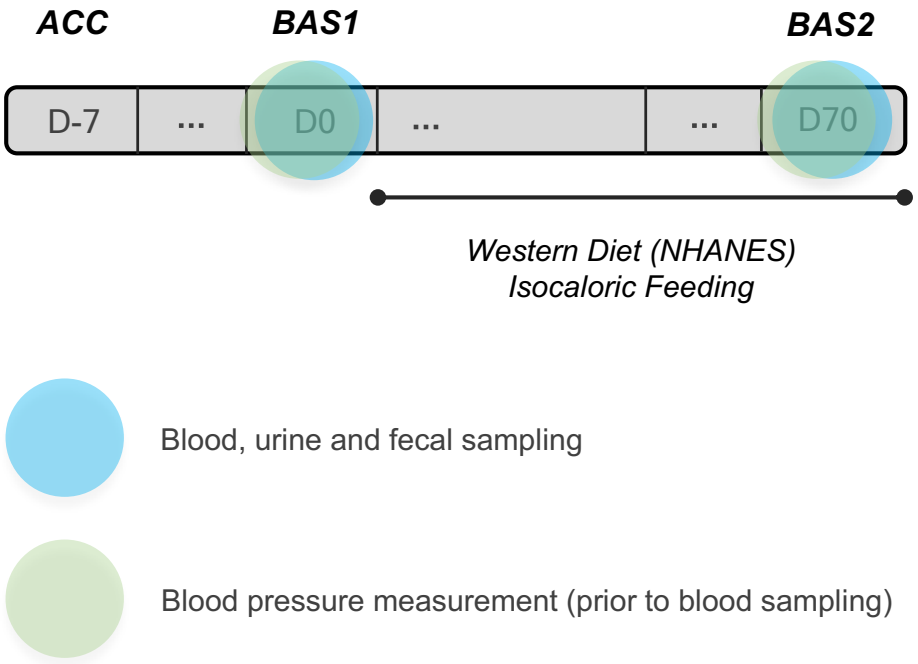

Figure 3. Temporal Changes in Standard Clinical Chemistry Parameters After Ten Weeks of Feeding with a High-Fat, High-Monosaccharide, Low-Fiber Western Diet. No notable alterations were observed in liver-related chemical parameters, such as ALT, ALP, albumin, and total protein, when comparing ***BAS1*** to ***BAS2***. Dogs at ***BAS2*** had decreased levels of serum bicarbonates, phosphorus, and potassium, but increased levels of chloride. There was also a reduction in BUN at ***BAS2***, along with an elevation in serum creatinine levels. Box plots represent the 25th, 50th and 75th percentile of the data ± 1.5 IQR (interquartile range). •: $0.01 < P \leq 0.05$; ••: $0.001 < P \leq 0.01$; •••: $P \leq 0.001$.

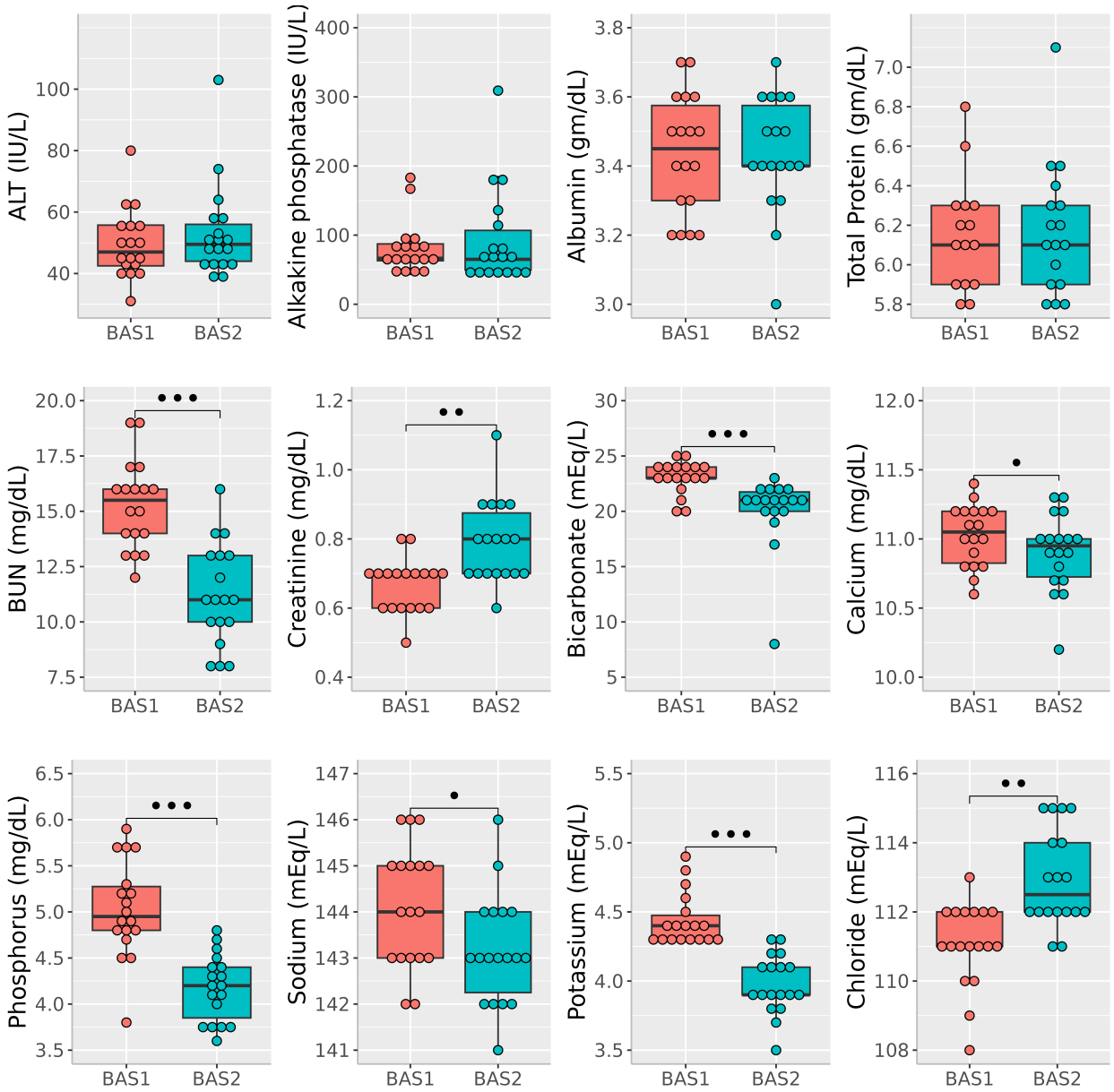

Figure 4. Temporal Changes in Fasting Blood Glucose, Serum Insulin and Glucagon After Ten Weeks of Feeding with a High-Fat, High-Monosaccharide, Low-Fiber Western Diet. The WD resulted in a significant 16.5% increase in fasting blood glucose, approaching the upper physiological limit. This was accompanied by a significant 36.2% decrease in insulin levels, and a trend towards lower serum glucagon levels which did not reach statistical significance. Box plots represent the 25th, 50th and 75th percentile of the data ± 1.5 IQR (interquartile range). •: 0.01 < P ≤ 0.05; •••: P ≤ 0.001.

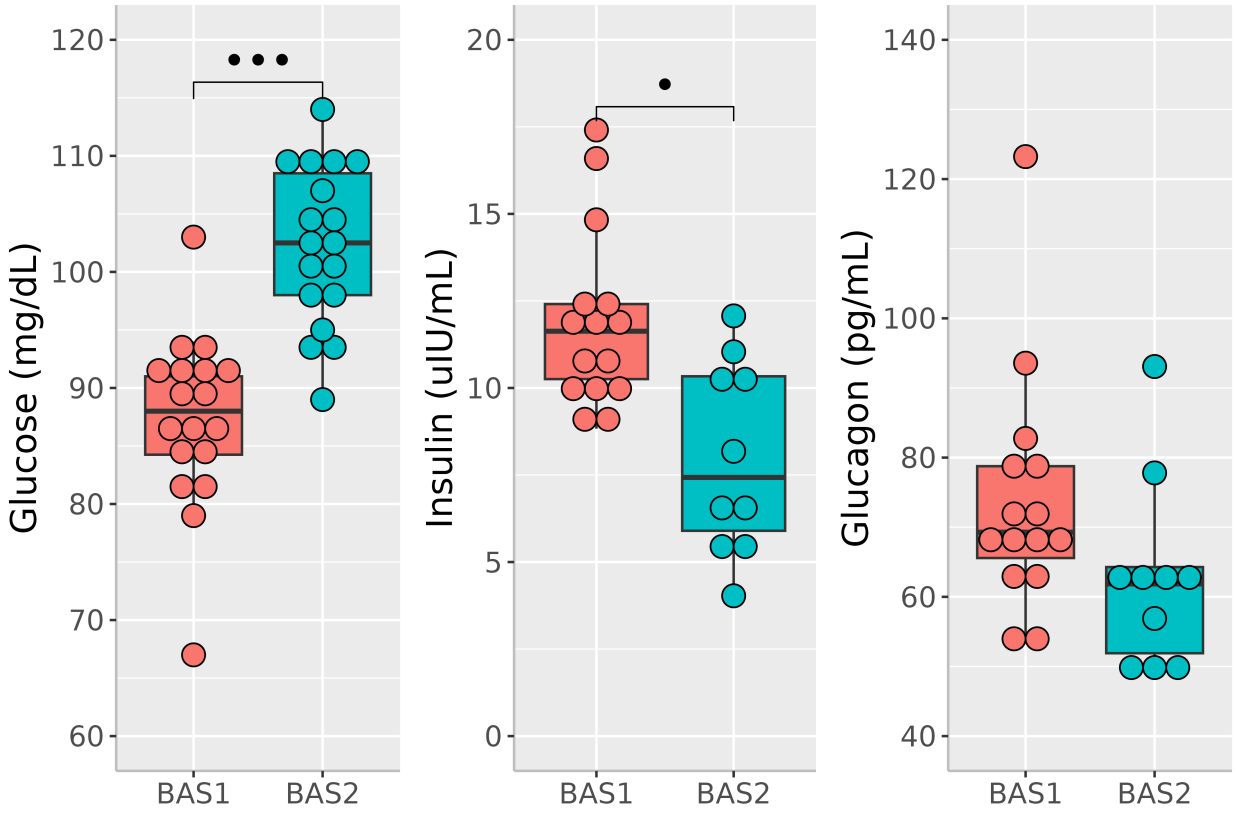

Figure 5. Temporal Changes in Systolic Blood Pressure After Ten Weeks of Feeding with a High-Fat, High-Monosaccharide, Low-Fiber Western Diet. Dogs fed a WD for ten weeks had significantly higher blood pressure measurements compared with baseline (***BAS1***). Measures were taken by a certified cardiologist using a Doppler device. To avoid bias in the recordings, these measurements were consistently taken before any blood was collected during each study period. To follow the ACVIM consensus panel guidelines for assessing hypertension (Acierno et al., 2018) and ensure accuracy, five consecutive and consistent SBP measurements were obtained from each subject. These values were then averaged to calculate an individual estimate of SBP. Box plots represent the 25th, 50th and 75th percentile of the data ± 1.5 IQR (interquartile range). •: $0.01 < P \leq 0.05$.

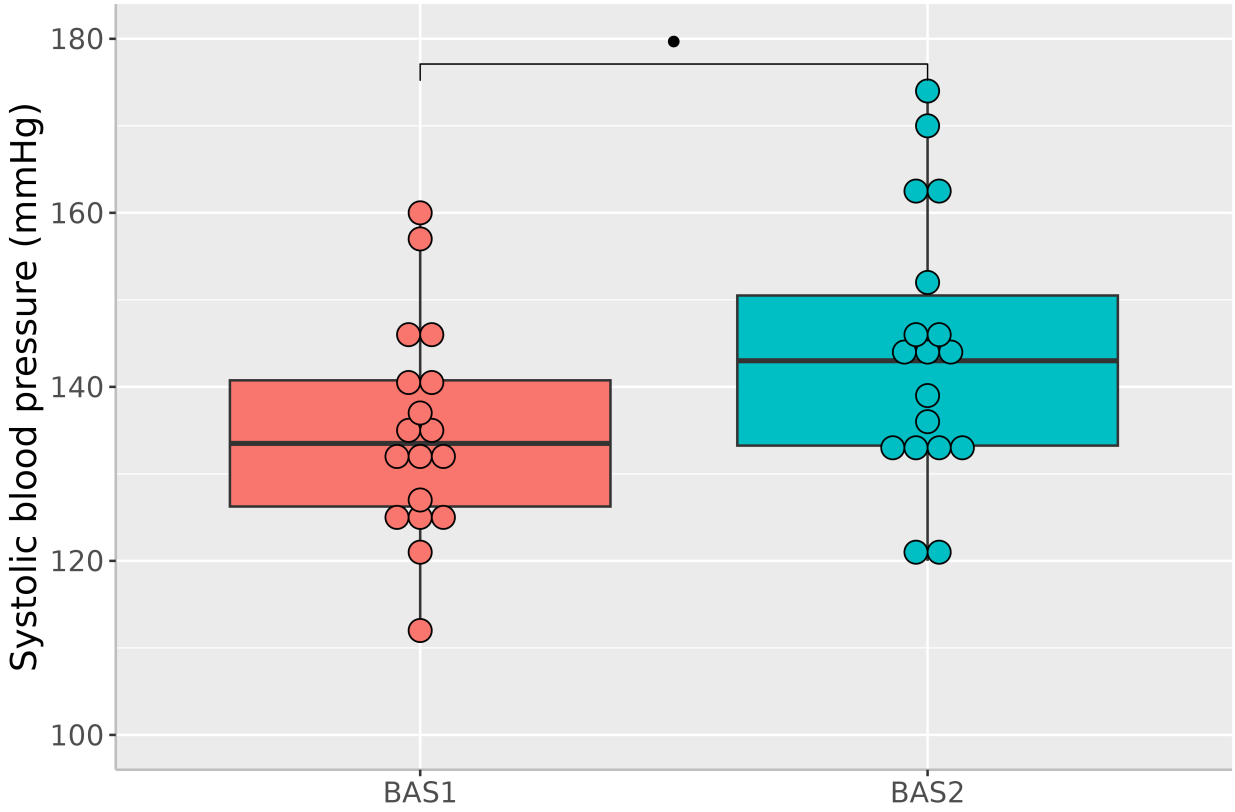

Figure 6. Temporal Changes in Total Cholesterol, HLD-Cholesterol and LDL-Cholesterol After Ten Weeks of Feeding with a High-Fat, High-Monosaccharide, Low-Fiber Western Diet. Circulating levels of cholesterol were significantly increased (+44.2%) after ten weeks of feeding with the isocaloric WD. Notably, this change was accompanied by a significant reduction in HDL-cholesterol and a 26.8% elevation in LDL-cholesterol. Box plots represent the 25th, 50th and 75th percentile of the data ± 1.5 IQR (interquartile range). •••: $P \leq 0.001$.

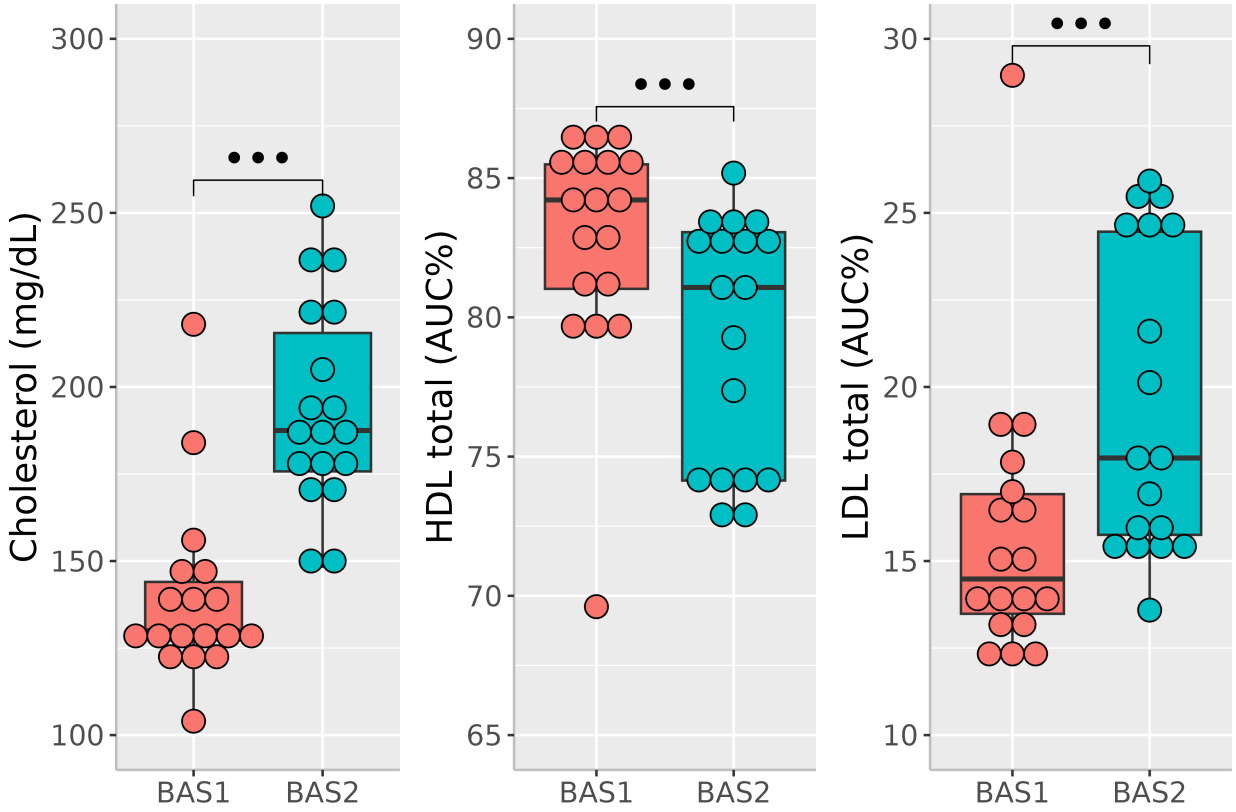

Figure 7. Temporal Changes in Antioxidant (A) and Oxidant (B) Stress Markers After Ten Weeks of Feeding with a High-Fat, High-Monosaccharide, Low-Fiber Western Diet. The WD had mild effects on antioxidant markers, with no significant changes in CUPRAC, FRAP, TEAC, and Thiol values. However, PON-1 levels significantly decreased at ***BAS2***. The impact of the WD on oxidative stress parameters was more consistent, with total oxidant status significantly increasing at ***BAS2***. The increase extended to reactive oxygen metabolites (d-ROMs). Conversely, there was a decrease in POX-Act post-WD, but no notable effects on AOPP. Box plots represent the 25th, 50th and 75th percentile of the data ± 1.5 IQR (interquartile range). •: $0.01 < P \leq 0.05$; ••: $0.001 < P \leq 0.01$; •••: $P \leq 0.001$.

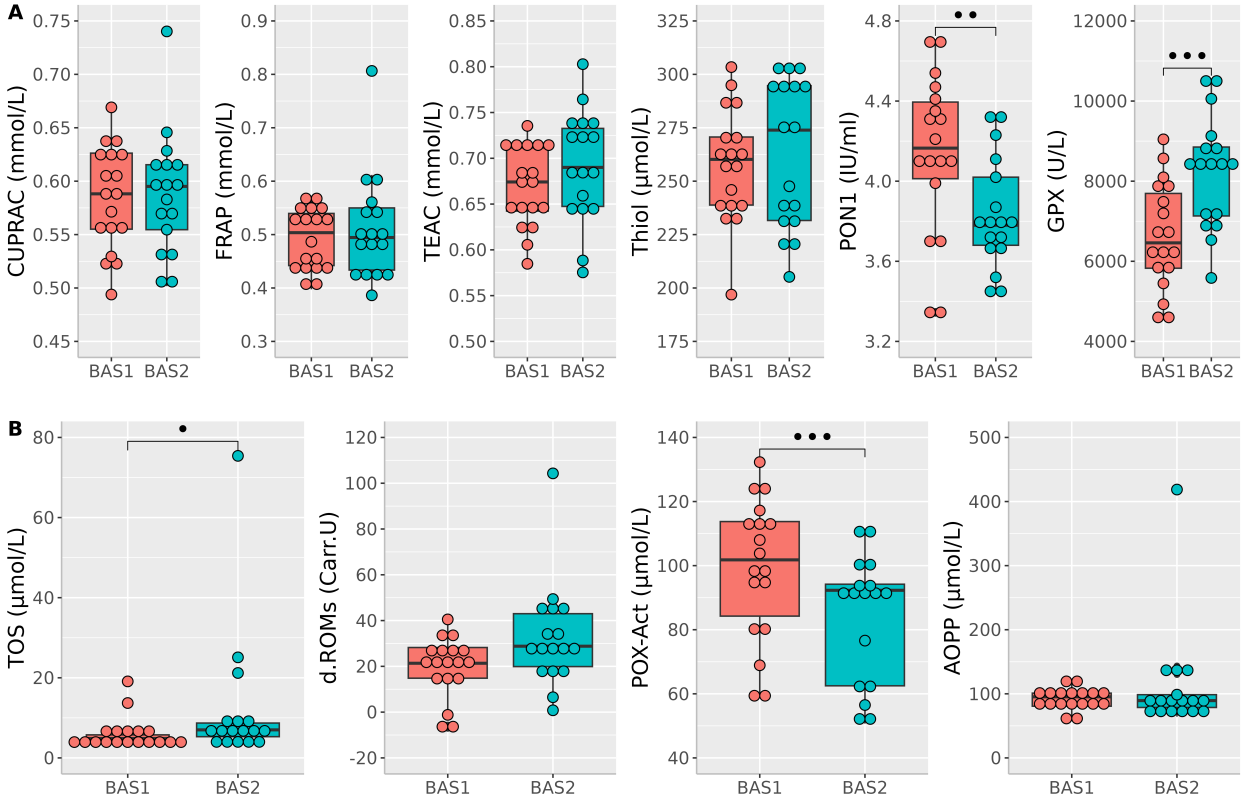

Figure 8. PCA scores plots (*General Metabolism*) of (**A**) Urine, (**B**) Stool, and (**C**) Serum *before* feature selection.

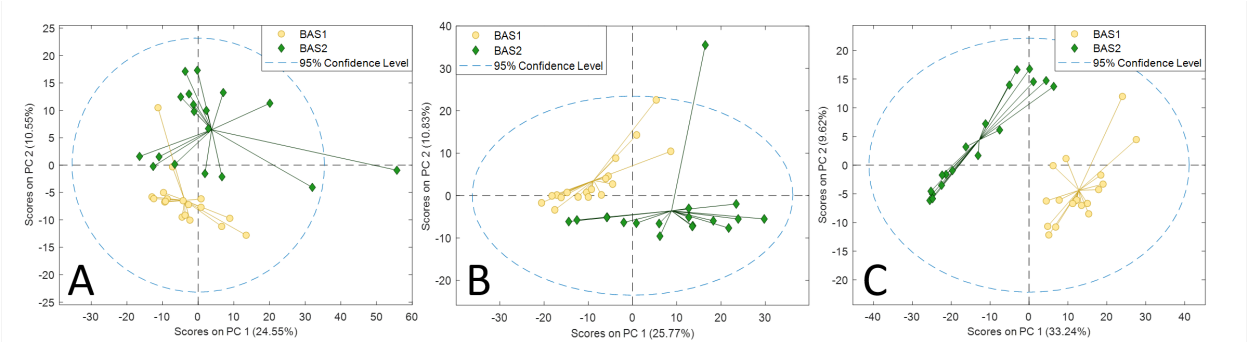

Figure 9. PCA scores plots (*General Metabolism*) of (**A**) Urine, (**B**) Stool, and (**C**) Serum *after* feature selection.

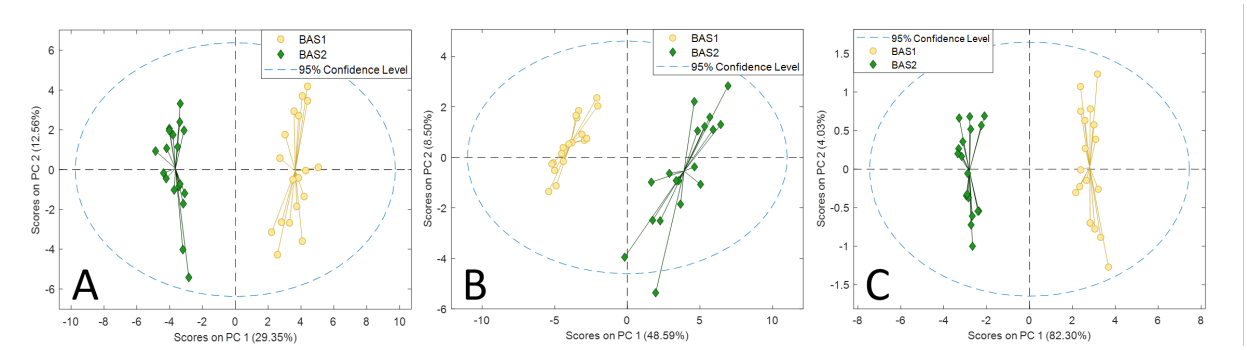

Figure 10. PCA scores plots (*Complex Lipids*) of (**A**) Urine, (**B**) Stool, and (**C**) Serum *before* feature selection.

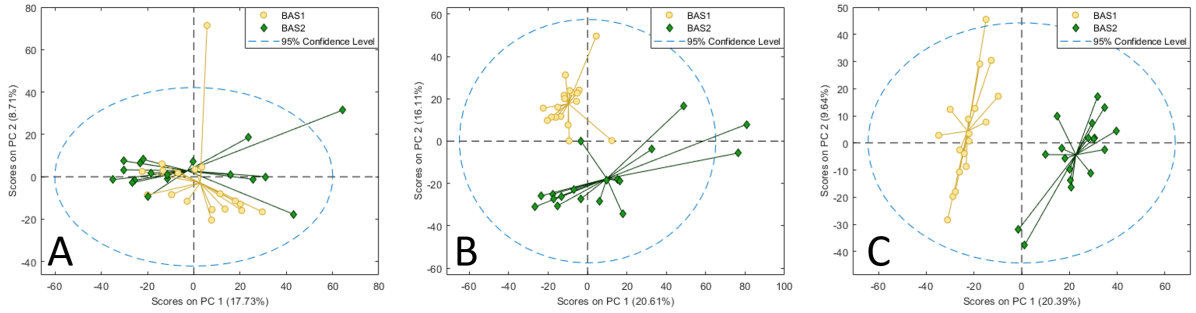

Figure 11. PCA scores plots (*Complex Lipids*) of (**A**) Urine, (**B**) Stool, and (**C**) Serum *after* feature selection.

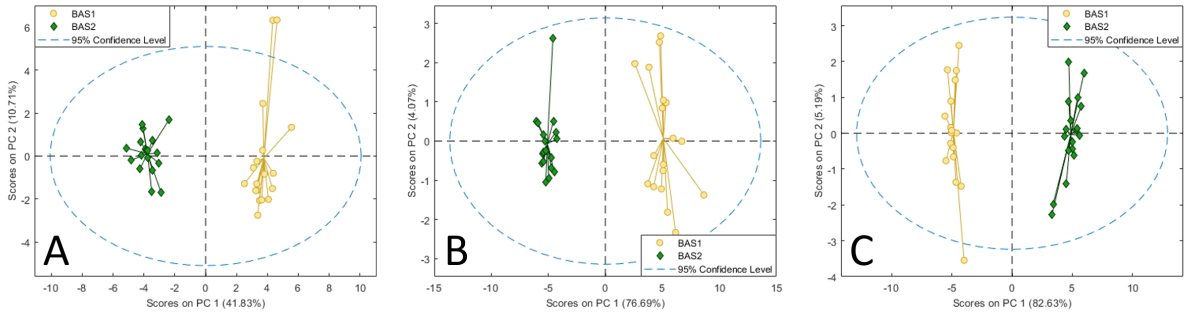

Figure 12. PCA scores plots (*Biogenic Amines*) of (**A**) Urine, (**B**) Stool, and (**C**) Serum *before* feature selection.

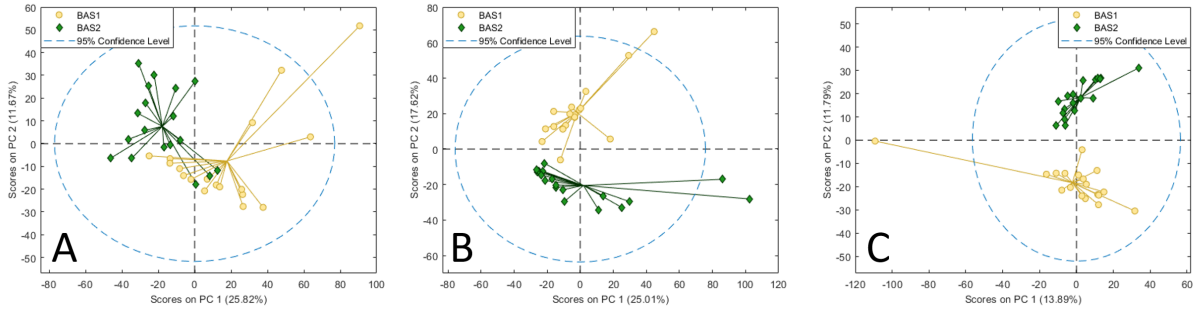

Figure 13. PCA scores plots (*Biogenic Amines*) of (**A**) Urine, (**B**) sSool, and (**C**) Serum *after* feature selection.